



## Mobile weather radar to provide intelligence on wildfire hazards

Adrien Guyot<sup>1,2</sup>, Hamish McGowan<sup>2</sup>, Jean-Baptiste Filippi<sup>3</sup>, Alberto Alonso-Pinar<sup>4</sup>, Alain Protat<sup>1</sup>,  
Nicholas McCarthy<sup>5</sup>, Simon Webster<sup>6</sup>, Amie Taylor<sup>6</sup>

5 <sup>1</sup> Australian Bureau of Meteorology, Melbourne, Australia

<sup>2</sup> Weather and Climate Science Research Alliance, The University of Queensland, Brisbane, Australia

<sup>3</sup> Centre National de la Recherche Scientifique, University of Corte, Corsica, France

<sup>4</sup> Aon Reinsurance Solutions, Paris, France

<sup>5</sup> Country Fire Authority, Victoria, Australia

10 <sup>6</sup> Queensland Fire Department, Queensland, Australia

*Correspondence to:* Adrien Guyot ([a.guyot@uq.edu.au](mailto:a.guyot@uq.edu.au))

**Abstract.** Extreme wildfire behaviour is increasingly associated with deep pyro-convection and pyro-cumulonimbus (pyroCb) development, posing challenges for both scientific understanding and operational wildfire management. Existing wildfire intelligence relies on a combination of aerial observations, satellite remote sensing, numerical weather prediction,  
15 and in-situ measurements, which can be limited in resolving rapidly evolving plume dynamics and near-fire wind changes. Portable weather radars represent a promising observational approach by providing high-resolution measurements of plume structure, kinematics, and microphysical properties, together with conventional radar products such as precipitation and outflow detection. However, their role within wildfire intelligence frameworks remains relatively unexplored.

In this study, we review two decades of portable radar observations of wildfires and prescribed burns and present new  
20 analyses from a recent deployment of a mobile dual-polarization X-band radar during an extreme wildfire in Eastern Australia. Building on these observations, we introduce a set of radar-derived diagnostics relevant to wildfire intelligence, including plume depth evolution, signatures of pyro-convective dynamics, detection of low-level wind changes, and indicators associated with transitions from pyro-cumulus to deep convection. These diagnostics complement existing satellite and modelling approaches by providing information on processes that are not directly observable from current operational  
25 platforms.

Using a Technology Readiness Level (TRL) framework, we assess the maturity of portable radar applications for wildfire monitoring. While fundamental aspects of pyrometeor scattering remain at low readiness (TRL 1–3), repeated field deployments indicate increasing maturity of plume observations (TRL 4–5), with some diagnostic products approaching pre-



operational capability. These findings suggest that further progress will depend not only on technical development but also  
30 on practical considerations such as deployment logistics, integration with existing systems, and operational evaluation.  
Overall, portable weather radar may provide an additional component of future multi-sensor wildfire intelligence systems,  
helping to bridge part of the observational gap between satellite remote sensing and fireground measurements while  
improving understanding of fire–atmosphere interactions.

## 1. Introduction

35 Wildfires are increasingly recognised as complex coupled fire–atmosphere systems capable of generating extreme  
convective phenomena that challenge both scientific understanding and operational wildfire management. In recent decades,  
the frequency and intensity of large fires have increased in many regions worldwide (Cunningham et al., 2024; Jones et al.,  
2024), driven by climate variability, fuel accumulation, and expanding human presence in fire-prone landscapes. Under  
favourable atmospheric and fuel conditions, intense fires can transition from surface-driven combustion to strongly buoyant  
40 convective systems capable of producing deep pyro-cumulus (pyroCu) and pyro-cumulonimbus (pyroCb) clouds. These fire-  
generated convective storms represent one of the most hazardous manifestations of wildfire behaviour because they can  
fundamentally alter local meteorology and create feedback that accelerate fire spread and unpredictability (Potter et al.,  
2012a, 2012b; McRae et al., 2015). Recent catastrophic wildfires in Hawaii (2023) (Mass and Ovens, 2024) and Southern  
California (2025) (Guirguis et al., 2025) have also highlighted the very hazardous impact of downslope windstorms  
45 (Abatzoglou et al., 2023), with extreme dry (foehn) winds causing elevated fire spread (McGowan et al., 2026).

PyroCb events in particular are associated with extreme updrafts, plume collapse (which remains a process to be quantified  
and understood), lightning generation, fire-induced vortices, and rapid wind changes at the fireground (Potter et al., 2012a,  
2012b; Peace et al., 2018, 2023). Such phenomena can produce erratic fire behaviour, including long-range ember transport,  
rapid flank runs, and sudden shifts in fire direction that pose severe risks to firefighting personnel and nearby communities.  
50 From an atmospheric perspective, pyroCb clouds inject smoke, ash, and trace gases into the upper troposphere and  
occasionally the lower stratosphere, influencing radiation budgets and regional air quality (Peterson et al., 2018; Christian et  
al., 2019). Despite their significance, the physical processes governing the initiation and evolution of extreme pyro-  
convection remain poorly constrained, largely because observations within and around active fire plumes are sparse.  
Additionally, traditional storms that are uncoupled to fires can also affect fire ground environments and produce hazardous  
55 conditions through thunderstorm outflows (McGowan et al., 2025).

Operational wildfire management currently relies on weather intelligence from a combination of numerical weather  
prediction, fire spread modelling (which itself relies on weather intelligence inputs), satellite remote sensing, in-situ  
observations such as automatic weather stations and radiosondes, and fireground or aircraft observer reports (visual and



photographs). In-situ measurements only capture the relevant information at a few locations and lack spatial coverage.

60 Satellite platforms provide broad spatial coverage and are essential for detecting fire radiative power, plume height, and cloud-top properties; however, their temporal resolution and sensitivity to obscuration by thick smoke or cloud can limit their usefulness for monitoring rapidly evolving plume dynamics (Liu et al., 2022; Carroll et al., 2024). Fire behaviour models including coupled fire–atmosphere simulations have advanced considerably, yet they still struggle to represent sub-kilometre-scale processes such as plume entrainment, and localized wind changes that often govern extreme fire behaviour

65 (Cruz et al., 2018; Campos et al., 2025). In particular, Cruz et al. (2018) highlight the uncertainty these models can have for various conditions, and the caution while using these operationally as predictive tools. Aircraft-borne passive remote sensing is actively used within fire agencies in countries like Australia, usually to map on-demand, the fire front at sub-meter resolution, using infrared mounted cameras. Such observation flights also record the events via photography and visual observations. Consequently, there remains a critical observational gap between large-scale satellite monitoring and the small-

70 scale processes driving hazardous pyro-convective events.

Weather radar offers a unique opportunity to bridge this gap by providing high-resolution measurements of plume structure, kinematics, and microphysical properties. Operational weather radar networks have occasionally detected wildfire smoke plumes and pyroCb clouds, demonstrating that radar backscatter from ash, debris, and hydrometeors can reveal key aspects of plume evolution (McCarthy et al., 2018; Guyot et al., 2023). Studies using S- and C-Band operational radars have

75 documented signatures such as enhanced reflectivity columns, divergent outflows, and rotation within pyro-convective storms. However, operational radar networks were not designed for wildfire monitoring and present several limitations. Their scanning strategies prioritise precipitation surveillance rather than low-level plume sampling, beam geometry often overshoots shallow plumes at long ranges, and spatial resolution is insufficient to resolve fine-scale turbulence and embedded updraft cores near the fire source. Wildfires often occur in complex terrain and operational weather radar are

80 especially subject to beam blockage by topography in these environments, thus obscuring from view critical fire-atmosphere and topography interactions. In addition, operational radars may be located hundreds of kilometres from active fires, reducing sensitivity to weak pyrometeor echoes and limiting the ability to capture the earliest stages of plume development.

To address these observational challenges, researchers have begun deploying portable weather radar systems capable of operating closer to wildfire environments (Wurman and Weygandt, 2003; McCarthy et al., 2018; Aydell and Clements,

85 2021; May et al., 2024; Sun et al., 2025; McGowan et al., 2026). Mobile X-, Ka-, and W-Band radars provide improved spatial and temporal resolution and can be positioned to optimize viewing geometry while maintaining safe operational distances from hazardous fire conditions. Although still relatively rare, these deployments have demonstrated the ability of portable radar platforms to capture plume dynamics, quantify updraft velocities, and investigate the microphysical properties of pyro-convective clouds. The following section provides a brief review of portable radar observations of wildfires and

90 prescribed burns reported in the literature.



Portable weather radar observations of prescribed burns or wildfires have been limited thus far, although the growing number of dedicated radar-based observation platforms is expected to lead to significant advancements in the next decade. Here, we provide an overview of all observations as reported in the scientific literature. Wurman and Weygandt (2003) reported the first-ever observations of wildfire smoke plumes with portable weather radars for two fires that occurred  
95 in the US, for which the authors deployed two Doppler on Wheels (DOW) X-Band radars. This conference presentation and subsequent conference paper presented only a few frames of reflectivity and Doppler velocity, and reported doppler velocities of 20 m/s in the plume. A decade later, Palumbo et al. (2013) presented observations of a wildfire smoke plume in southern Australia using an experimental phased array portable X-Band radar. The observations reported in this conference paper and in Palumbo's PhD thesis (Palumbo, 2016) were also limited to a few frames from a low-intensity prescribed burn.  
100 These two pioneering opportunistic studies demonstrated both the feasibility of deployment and the sensitivity of X-Band radar to detecting pyrometeors, even for weak pyrometeors' plumes.

McCarthy et al. (2018) at The University of Queensland, in Australia, conducted the first dedicated campaign of wildfire pyrometeors' plume and cloud observations using a mobile X-Band radar, named the Bushfire Convective Plume  
105 Experiment (BCPE). The X-Band mobile platform was initially developed to study coastal convection on the Australian East Coast (Soderholm et al., 2016). While the platform remained unchanged for the BCPE, the deployment logistics were adapted to meet the safety requirements and the need for rapid deployment in response to rapidly evolving and hazardous fire-atmosphere conditions, along with the complexity of ongoing firefighting operations. These deployment conditions, as well as the radar at the core of the observational platform, are described in detail in McCarthy et al. (2018). The solid-state  
110 Furuno X-Band WR2100 radar has dual-polarization capability, allowing the reception of echo signatures in both vertical and horizontal channels. Observations from three wildfires in southeast Australia are presented in McCarthy et al. (2018), illustrating that the radar frequency was well-suited to capturing echoes from wildfire pyrometeors' plumes even at mid-range (20 km from the radar), despite the relatively low sensitivity of the solid-state radar at such distances. The Mt Bolton wildfire observations (McCarthy et al., 2018) captured a wildfire exhibiting extreme pyro-convective activity. The radar,  
115 operating in Range Height Indicator (RHI) mode, captured the cross-section of a turbulent pyrometeors' plume topped by pyro-Cumulus clouds that reached approximately 6 km in height. The polarimetric radar observations resolved vorticity structures in the plume, as shown by Doppler velocities, as well as pulsing and core convective updrafts in the reflectivity field. Subsequent analysis of the polarimetric variables using a dedicated clustering algorithm (McCarthy et al., 2020) identified various pyrometeors' sizes and shapes and their movement. This dataset remains the most comprehensive and  
120 high-resolution set of pyro-convective plume observations to date. Using the same UQ-XPOL platform and deployment strategy, McCarthy et al. (2023) presented observations of a wildfire-triggered thunderstorm in Eastern Australia. At the extended range it was operating, the radar lacked the sensitivity to detect pyrometeors' echoes but successfully captured the lifecycle of a short-lived pyroCb. The authors operated the radar in Plan Position Indicator (PPI) mode to capture the full volume of the thunderstorm. That study was innovative in combining geostationary satellite observations, wildfire spread



125 simulations, and radar observations, which together demonstrated the simultaneous occurrence of a crown fire and the formation of the pyroCb.

Aydell and Clements (2021) present a new dedicated platform developed by San Jose State University, with a solid state, low power Ka-Band radar mounted on the back of a 4WD utility vehicle. They follow a similar deployment strategy as in  
130 McCarthy et al. (2018) and Lareau and Clements (2016), similar to the DOW. The authors operated both in PPI and RHI modes, adapting to the most suitable strategy depending on radar and plume respective locations and terrain obstructions. They present observations from two wildfires and a controlled burn in California and Utah, capturing reflectivities ranging to  $-15$  to  $20$  dBZ, a similar range of reflectivities as observed by UQ-XPOL (McCarthy et al., 2018) for wildfires of the same intensity. This illustrates that the scattering mechanism at Ka-Band for pyrometeors is somehow similar to that at X-Band  
135 frequency. In Kingsmill et al. (2023), the authors present observations from a W-Band doppler radar mounted on the University of Wyoming research aircraft. The aircraft flew into smoke plumes and clouds generated by pyro-convective activity from the Pioneer fire near Boise, Idaho. The doppler radar recorded maximum updrafts of  $36$  m/s and enabled for the first time to sample ash particles in-situ. Measured reflectivities at W-Band only reach maximum of  $-5$  to  $0$  dBZ, while the ground-based S-Band radar recorded reflectivities of up to  $25$  dBZ for that same pyro-convective cloud. This very significant  
140 offset between the two radars illustrates most likely fundamentally different scattering mechanisms of ashes at W- and S-Bands, unlike other frequencies where authors have reported similar reflectivity values for the same fires at X- and S-Bands (Rogers et al., 1997; McCarthy et al., 2018, 2019). At W-Band frequency, scattering is non-Rayleigh, where the size of the scatterers is typically similar to or larger than the radar wavelength. Collocated W-Band frequency observations with X- or S-Band frequency radars would help better understand the nature of the scatterers, but no such study has been conducted to  
145 date. Lareau et al. (2024) designed an experimental setup including two lidars and a Ka-Band radar to observe a high-intensity prescribed fire in Utah. The collocated Ka-Band KASPR with one lidar allowed to compare scattering properties from the same regions of the plume and clouds between the radar frequency and the near visible of the lidar. It illustrated for the first time that while the lidar clearly distinguished the condensation level: the lidar attenuated backscatter almost completely attenuates past the condensation level since droplets strongly attenuate in the near visible spectrum. On the other  
150 hand, the radar data showed a continuum in its reflectivity and polarimetric variables, demonstrating that droplets at these levels are probably of small size and in minority compared to the pyrometeors in larger concentration and/or larger sizes. This study also illustrated that pyro-convective microphysics remains very poorly understood (as already described in McCarthy et al., 2018): the nature of the pyrometeors, their dielectric properties, size sorting and interaction with water as vapor, liquid or ice, and the role of fine particles in nucleation and droplet formation present challenges to model and parameterise given the complexity of concomitant processes. These observations in Lareau et al. (2024) also provided quantitative estimates of the wind velocity within the plume, with a very strong central updraft of  $35$  m/s, strong rotation of the plume ( $s^{-1}$ ) and the pulsing mechanism leading to the deepening of the plume and associated pyrocumulus. Finally, the most recent addition to the literature is from May et al. (2024), where authors reported observations from a prescribed burn



160 observed by an off-the-shelf (integrated trailer for towing behind a light truck) Leonardo Meteor 50 X-Band weather radar in WA. In this study, the authors presented the capability of that radar to observe a wind change over the fire ground in clear air conditions, owing to the high sensitivity (-5 dBZ) of the radar at that range (10 km). May et al. (2024) uses that data to explore and estimate the accuracy of polarimetric variables, a critical information for the interpretation of wildfire echoes at various frequencies.

165 In summary, over the last 20 years or so, five different research groups in the United States of America and Australia have operated portable radars, for the majority mounted on the back of small trucks or 4WD, or trailers, with one exception with the airborne W-Band mounted on a research aircraft. Most groups chose X-Band frequency, due to the smaller size of the antenna, as compared to S- or C-Band radars. Two of the radars are solid state radars (UQ XPOL from The University of Queensland, and KASPR from San Jose State University), offering lower power consumption but a degraded sensitivity compared to conventional radar technologies based on klystron or magnetrons (DOW or Monash Leonardo X-Band radar).  
170 Despite that lower sensitivity, both UQ-XPOL and KASPR demonstrated their capability to observe high resolution pyro-convective plume and clouds, while maintaining operational safety distances to observed wildfires. The research groups operated both in PPI and RHI modes depending on the radar location in relation to the fire, as well as other considerations based on processes observed in the plume and clouds.

175

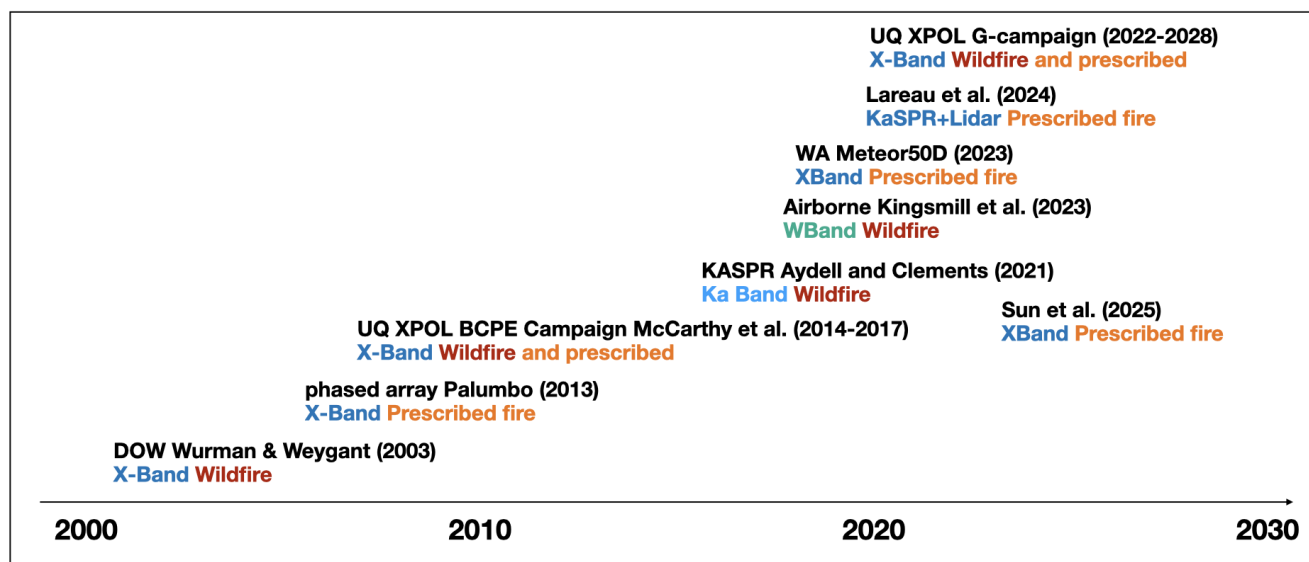


**Figure 1.** Timeline of major portable weather radar deployments at wildfire or prescribed fires as reported in the literature.

These studies demonstrated: (i) the feasibility to operate radars at safe distance and acceptable risk to often very dangerous  
180 wildfires; (ii) to collect data that proved essential to build an understanding of the processes underpinning pyro-convection



and downslope windstorm; (iii) to quantitatively link step changes in fire behaviour to increased pyro-convective activity; (iv) to demonstrate the capability to quantitatively and spatially measure at high-resolution phenomena such as wind change, updrafts, downdrafts, firebrand identification and transport. Based on the above, we believe that the use of portable weather radar to gather observations of environmental conditions around wildfires has reached a new level of maturity. This leads to two essential questions: (1) is science and technology ready to be used as part of a new toolkit to augment wildfire intelligence? ; (2) how could it support existing tools already used by fire agencies, such as fire behaviour models, satellite remote sensing of fire radiative power, hyperspectral imagery or deployable AWS and atmospheric soundings?

In this paper, we provide key elements to answer the first question, and provide some elements to explore the second question. We use recently collected data at a large wildfire in Eastern Australia to demonstrate the feasibility to produce portable radar-derived products that could be used by fire agencies. We develop a road map from research to operations, assess the development stages of the technology using the Technology Readiness Level (TRL) framework, and make recommendations for the future work.

## 2. Operational constraints and observational requirements

Wildfire management operates under rapidly evolving environmental and safety constraints that impose specific requirements on observing systems intended to support decision-making. Eruptive fire behaviour can develop on timescales of minutes, often in complex terrain and under limited visibility due to smoke. Consequently, an observing platform designed to augment wildfire intelligence must be capable of operating at safe stand-off distances or from aircraft while resolving sub-kilometre plume structure and detecting rapid dynamical changes such as wind shifts and convective intensification. In this section, we outline key operational needs that motivate the development of portable weather radar applications.

### 2.1 Fireground constraints

Wildfire environments impose a set of operational constraints that fundamentally differ from those encountered in conventional meteorological observing campaigns. Any observing system intended to operate in proximity to active fires must prioritise personnel safety, maintain flexibility under rapidly evolving conditions, and integrate within complex incident management structures. These constraints shape not only what can be observed, but also when and how observations can realistically be conducted.

A primary fireground constraint is the requirement to maintain safe stand-off distances from active fire fronts and areas of potentially rapid fire spread. Experience from dedicated wildfire observation campaigns, such as the BCPE, demonstrated



210 that observing platforms must be positioned with careful consideration of forecast fire behaviour, plume advection, terrain  
accessibility, and available evacuation routes. Fireground conditions can deteriorate rapidly due to changes in wind, spotting  
activity, or plume collapse, necessitating conservative site selection and the ability to withdraw quickly if conditions  
escalate.

Wildfires are also characterised by rapid temporal variability, with transitions in fire behaviour and plume dynamics  
215 occurring on timescales of minutes. This volatility constrains the operational window available for observations and places  
strong emphasis on rapid mobilisation and readiness. Observing teams must be capable of responding quickly to emerging  
fire–atmosphere coupling while accepting that opportunities for sustained observations may be limited or abruptly  
terminated by safety considerations.

Another key constraint arises from the need to operate within active incident management frameworks. Firegrounds are  
220 highly regulated environments where access, movement, and communication are controlled by appropriate operational  
supervision. Observational activities must therefore be coordinated closely with or by fire agencies to ensure alignment with  
safety briefings, exclusion zones, and suppression operations. This coordination is essential not only for safety but also to  
ensure that observations are collected in a manner that is compatible with operational priorities on the fireground. The  
correlation between events with eruptive fire behaviour and events where fire agencies can support supervision is ultimately  
225 low.

Finally, wildfire environments impose significant logistical and environmental constraints. Observations are often conducted  
in remote or rugged terrain, under conditions of heavy smoke, elevated temperatures, and limited infrastructure. Power  
supply, communications, vehicle access, and personnel endurance all place practical limits on the duration and complexity of  
field operations. These factors collectively constrain the type and volume of data that can be acquired and highlight the  
230 importance of designing observing systems and workflows that are robust, mobile, and operationally simple.

Taken together, these fireground constraints underscore that the successful use of portable weather radar in wildfire  
environments depends not only on technological capability but also on the ability to operate safely, flexibly, and  
cooperatively within complex and hazardous operational contexts. These considerations motivate the radar-specific  
requirements outlined in Section 2.2.

## 235 **2.2 Radar-specific requirements**

The operational constraints outlined in Section 2.1 and the observational gaps described in Section 2.2 define a set of  
requirements that an observing system must satisfy to meaningfully augment existing wildfire intelligence tools.



240 A primary requirement is the ability to resolve plume structure and dynamical evolution at high spatial and temporal resolution. Rapid transitions in pyro-convective activity frequently occur on timescales shorter than those captured by satellite observations or conventional field measurements. An observing system must therefore be capable of capturing vertical plume growth, structural pulsing, and localized kinematic signatures associated with rapidly evolving fire behaviour.

Another key requirement is the capability to detect wind changes and boundary-layer structures in environments with limited or no precipitation. Many hazardous fire behaviour events are driven by low-level wind shifts, convergence lines, or fire-induced circulations that may not be detectable through traditional meteorological observations alone.

245 In addition, established meteorological requirements for weather radar remain highly relevant for fire operations. These include: (i) the capacity to observe and quantify precipitation over the fireground and detect dry lightning occurrence; and (ii) the ability to assess post-storm environmental conditions that determine the safe deployment of aerial assets, including fixed-wing aircraft and helicopters transporting personnel.

250 Integration with existing wildfire intelligence systems represents a further requirement. Radar observations must complement satellite remote sensing, numerical modelling, and in-situ measurements, providing information that bridges the scale gap between regional monitoring and fireground processes.

Finally, wildfire applications require observations that can be translated into clear and operationally interpretable diagnostics rather than raw meteorological variables alone. Indicators of plume deepening, rapid structural reorganization, or emerging dynamical features are particularly relevant for situational awareness and decision-making in operational environments.

255 Taken together, these requirements provide a framework for evaluating portable radar deployments within wildfire environments. Section 3 describes how portable weather radar systems are typically configured to address these needs.

### **3. Portable radar deployment and dataset**

260 Portable weather radar deployments for wildfire observation are shaped by the operational requirements outlined above but can be implemented using a range of radar frequencies, scanning geometries, and hardware architectures. Rather than being tied to a single instrument design, wildfire radar deployments reflect a broader observational design space defined by trade-offs between mobility, sensitivity, and spatial resolution.



### 3.1 Radar platform and scanning strategy

Building on the radar-specific requirements outlined in Section 2.2, portable weather radar deployments for wildfire observation operate across a range of frequencies, scanning configurations, and hardware architectures, each reflecting trade-offs between mobility, sensitivity, and observational flexibility.

Radar frequency plays a central role in defining observational capability. Compact X-Band radars have the advantage of relatively small antenna size and portability, allowing high-resolution sampling of plume structure while maintaining sufficient sensitivity to detect weak echoes from smoke, ash, and small hydrometeors. Ka- and W-Band systems offer enhanced sensitivity to fine particles and microphysical processes but may experience stronger attenuation and reduced range, particularly in dense smoke or precipitation. Lower-frequency systems provide greater penetration but are generally less suited to rapid deployment due to their larger size and logistical demands such as access to high voltage power supply. Another consideration to take into account is that for higher frequency radars, the Nyquist velocity is lower for the same maximum range (the so-called doppler dilemma), making doppler measurements more difficult to unfold and requiring more aggressive ratios for dual-PRF (Pulse Repetition Frequency) techniques. The diversity of frequencies used in recent wildfire studies (Table 1) reflects differing scientific priorities, ranging from plume kinematics to microphysical characterisation.

Scanning strategies must balance the need to resolve vertical plume development with broader situational awareness of plume evolution within the ambient flow. Range–Height Indicator (RHI) scans are frequently employed to capture cross-sections of plume structure, enabling analysis of plume depth, tilt, and embedded dynamical features such as updraft cores or rotational signatures. Plan Position Indicator (PPI) scans provide complementary horizontal context, revealing plume extent, evolving boundaries, and interactions with the surrounding wind field. Effective wildfire radar deployments therefore often combine multiple scanning modes, adapting observational focus as plume geometry and fire behaviour evolve.

Hardware architecture also influences deployment strategy. Solid-state transmitters offer advantages in terms of power efficiency, reliability, and rapid start-up, making them well suited to remote field operations. Traditional high-power transmitters may provide improved sensitivity at longer ranges but require greater logistical support. These considerations highlight that portable radar deployment is not defined by a single optimal configuration but rather by a set of operational trade-offs shaped by fireground constraints and observational objectives.

An ideal compromise would sit with a good sensitivity at mid range (50 km) while retaining small size, low power consumption and robustness: this could be achieved by improving specifications of solid state radars like the WR2100, such as a higher transmitted power, or enhanced signal processing, or by using a magnetron or klystron radar with lower transmitted power than the Leonardo 50D.



**Table 1.** Radar specifications of mobile (all ground-based except for the WCR) platforms used for monitoring wildfire smoke plumes and clouds.

	DOW	UQ XPOL	KASPR	AARC RaXPOL	Monash XPOL	Wyoming Cloud Radar (WCR)
<b>Manufacturer and model</b>	Custom built (research instrument)	Furuno WR2100	Prosensing Inc.	Custom built (research instrument)	Selex/Leonardo 50D	Prosensing Inc.
<b>Technology and frequency</b>	Magnetron X-Band	Solid state X-Band	Solid state Ka-Band	TWTA X-Band	Magnetron X-Band	Klystron W-Band
<b>Beam width</b>	0.93 degree	2.7 degree	0.31 degree	1.0 degree	1.3 degree	0.5 or 0.7 degree
<b>Peak power</b>	250 kW	100 W	10 W	10 kW	75 kW	1.8 kW
<b>Pulse width</b>	~0.3–2 $\mu$ s	0.5–50 $\mu$ s	~0.05–0.5 $\mu$ s	~0.5–2.0 $\mu$ s	~0.3–2 $\mu$ s	100 ns to 500 ns
<b>PRF</b>	~300–1200 Hz	~300–2000 Hz	~1000–3000 Hz	~300–2000 Hz	~300–1200 Hz	1 kHz to 20 kHz
<b>Estimated sensitivity (depends on configuration)</b>	-10 to 0 dBZ at 50 km	22 dBZ at 50 km	14 dBZ at 20 km	-10 to 0 dBZ at 50 km	-10 to 0 dBZ at 50 km	-35 dBZ at 1km
<b>Reference in the scientific literature</b>	Wurman and Weygant (2003)	McCarthy et al. (2018, 2023); McGowan (2025, 2026).	Aydell and Clements (2021)	Sun et al. (2025)	May et al. (2024)	Kingsmill et al. (2023)

Together, these factors define a flexible observational framework in which portable weather radar can be configured to capture both the dynamical and microphysical characteristics of wildfire plumes. The following sections describe how these general principles were implemented during a recent deployment in Eastern Australia.

295



### 3.2 Deployment logistics and safety considerations

Portable weather radar deployments in wildfire environments are shaped not only by technical capabilities but also by operational logistics and safety constraints associated with active firegrounds. While specific implementations vary between research groups and radar platforms, several common principles have emerged from past deployments that influence site selection, coordination with fire agencies, and overall observational strategy.

**Site choice.** Selecting a suitable deployment location is a critical component of portable radar operations in wildfire environments (McCarthy et al., 2018). Sites must provide adequate visibility of the plume ideally to low levels while maintaining safe stand-off distances from active fire fronts and areas of potential rapid fire spread. Terrain, access routes, and anticipated plume advection all influence site choice, as line-of-sight limitations and beam blockage can significantly affect the quality of radar observations. In practice, deployment locations often represent a compromise between optimal viewing geometry and operational safety, particularly in rugged terrain where access may be restricted.

Another consideration is the need to maintain flexibility as fire behaviour evolves. Portable radar deployments frequently rely on road-accessible locations that allow repositioning if wind direction changes or plume development shifts relative to the radar. The ability to operate from elevated terrain or open clearings can improve sampling of vertical plume structure while reducing ground clutter, although such locations must be balanced against safety requirements and evacuation logistics. McCarthy et al. (2018) describes these procedures established and used for the Bushfire Convective Plume Experiment field campaign of 2015-2017.

Environmental conditions also play a role in deployment planning. Smoke density, heat exposure, and limited infrastructure can constrain the duration and complexity of operations, requiring teams to consider power supply, communications, and personnel safety when selecting deployment sites. These logistical factors often dictate operational decisions as strongly as purely observational objectives.

**Operators safety and Personal Protective Equipment (PPE).** As seen in figure 2, as part of the operative procedure, the team at UQ wore fire resistant protective equipment while attending the wildfire of Mt Bolton. Personal protection fire blankets and FFP2 masks were also accessible in the vehicle in case of need. For prescribed fires or while operating in a safer environment, crews may not use such equipment, as seen in figure 1a.

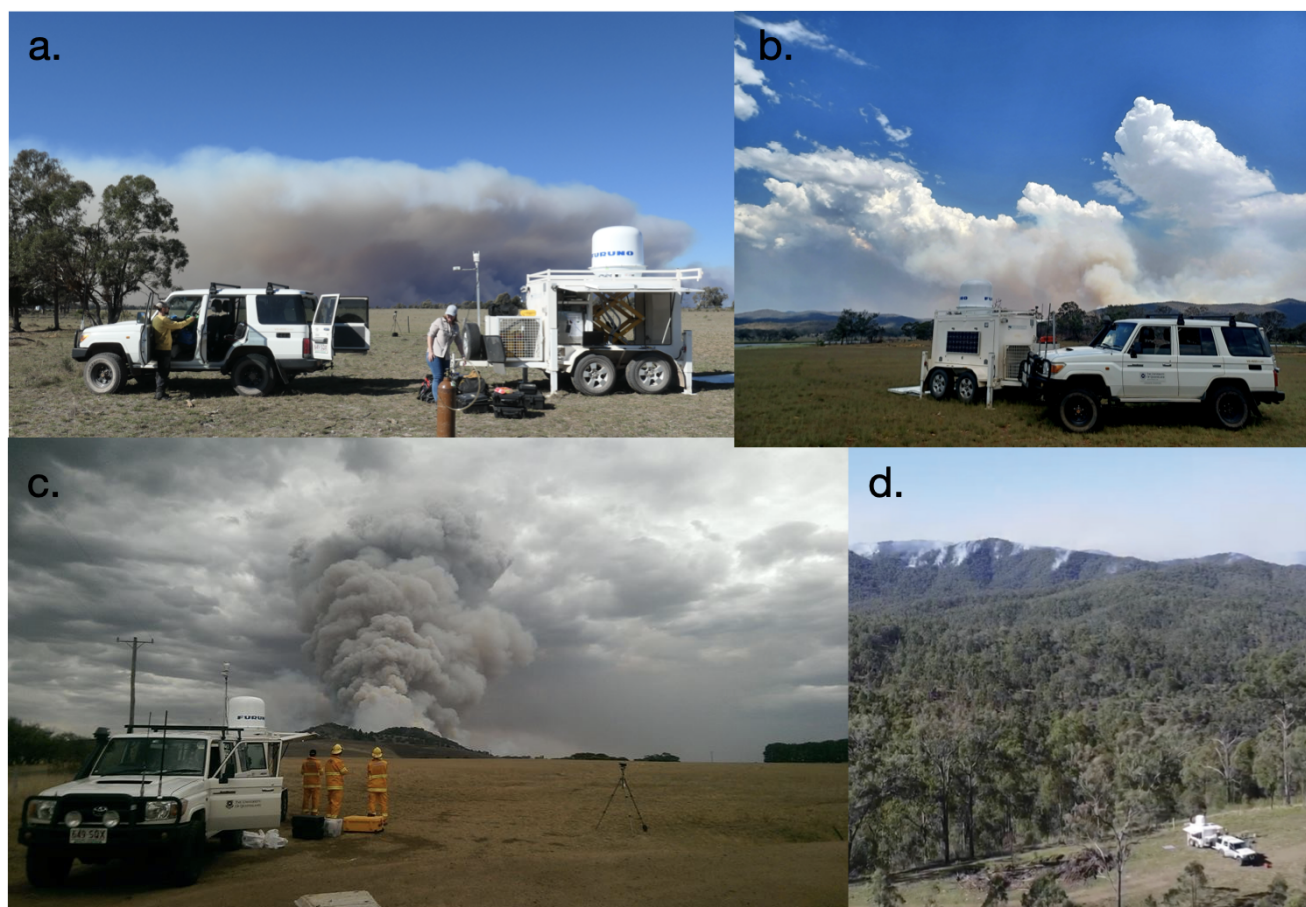


**Figure 2.** Examples of deployment of UQ XPOL radar to prescribed fires at (a) Moonie in Queensland, Australia (credits: Kathryn Turner) (a), and (d) D’Aguilar Range in Queensland, Australia (credits: Adrien Guyot); and wildfires at (c) Mt Bolton in Victoria, Australia (McCarthy et al., 2018) (credits: Nicholas McCarthy), and (b) Wallangara in Queensland, Australia (McGowan et al., 2026) (credits: Hamish McGowan).

325

**Fire agency coordination.** Effective portable radar deployment requires close coordination with fire management agencies and incident control teams. Wildfire environments are highly regulated operational spaces, and access to deployment areas typically depends on compliance with safety briefings, communication protocols, and evolving incident priorities. Collaboration with fire behaviour analysts and meteorological officers allows radar operators to identify periods of elevated fire–atmosphere coupling and to position observing systems in locations that complement existing monitoring efforts.

330

Coordination also ensures that radar operations do not interfere with suppression activities or aircraft operations. Deployment teams must remain aware of exclusion zones, changing access restrictions, and potential hazards such as falling



debris or rapid changes in fire behaviour. Regular communication with incident command structures enables radar observations to be conducted safely while maintaining awareness of operational developments on the fireground.

335 Beyond safety considerations, agency coordination can enhance the scientific and operational value of radar observations. Integrating radar deployments with existing data streams, including satellite monitoring, automatic weather stations, and fire behaviour modelling, facilitates interpretation of radar signatures within a broader wildfire intelligence framework. This collaborative approach reflects the multidisciplinary nature of wildfire monitoring and highlights the importance of embedding portable radar observations within established operational contexts.

#### 340 **4. Radar-derived diagnostics relevant to wildfire intelligence**

Portable weather radar observations collected over the past two decades have revealed a range of diagnostic signatures relevant to wildfire intelligence. Rather than focusing on a single deployment, this section synthesises radar-derived diagnostics reported across multiple portable radar studies and illustrates how these observations can be translated into physically meaningful indicators of plume dynamics, convective evolution, and near-fire wind behaviour. Examples are  
345 drawn from previously published deployments as well as representative observations to illustrate general concepts.

##### **4.1 Radar echo classification and segmentation**

A fundamental challenge in the interpretation of wildfire radar observations is the coexistence of multiple echo sources within a single scene, including pyrometeors, hydrometeors, clear-air returns, and various forms of clutter. Before higher-level diagnostics such as plume dynamics or convective evolution can be derived and interpreted, it is therefore necessary to  
350 first distinguish between these echo types in a physically meaningful way. Echo classification represents a foundational diagnostic step that enables portable weather radar observations to move beyond simple plume detection toward quantitative analysis of fire–atmosphere interactions.

Segmentation of radar echoes in wildfire environments is particularly challenging because polarimetric radar variables associated with different echo sources often overlap substantially. For example, correlation coefficient and differential  
355 reflectivity signatures of pyrometeors, clear-air returns, and clutter can occupy similar regions of phase space, making traditional threshold-based approaches unreliable. Recent work has shown that incorporating spatial texture information derived from gray-level co-occurrence matrices (GLCMs) can significantly improve discrimination between echo classes by capturing structural differences in radar imagery that are not evident in single-point measurements (Guyot et al., 2023). When combined with probabilistic clustering approaches such as Gaussian mixture models, these texture-based fields enable



360 segmentation of radar scenes into physically interpretable categories including pyrometeor plumes, precipitation, clear air,  
and clutter.

An important aspect of this approach is the preservation of the radar's native spherical geometry during processing. Performing segmentation directly within polar coordinates reduces range-dependent biases and ensures that classification reflects the true spatial structure of wildfire plumes, whose apparent scale varies strongly with distance from the radar.

365 Range-adaptive windowing strategies have also been shown to improve classification robustness by accounting for beam broadening effects that influence the statistical properties of radar textures at increasing range.

Among the polarimetric variables examined in previous studies, the contrast of the correlation coefficient together with dual polarimetric variables and reflectivity have emerged as one of the most discriminating features for separating pyrometeors from other echo sources, particularly when combined with texture metrics. While precipitation echoes tend to exhibit  
370 consistently high correlation coefficient values, pyrometeor plumes display broader variability associated with turbulent mixing and heterogeneous particle composition. These differences provide a physically grounded basis for automated segmentation and support the development of diagnostic products that isolate fire-generated particles within complex radar scenes.

Rather than representing a single algorithmic solution, echo segmentation should be viewed as a general interpretative  
375 framework that enables subsequent analysis of plume structure, kinematics, and convective evolution. By distinguishing between pyrometeors and meteorological echoes, segmentation provides a consistent foundation for comparing observations across portable radar deployments operating at different frequencies and configurations. In the following sections, we build upon this framework to examine how classified radar echoes can be used to infer plume development, dynamical signatures, and indicators of escalating pyro-convective activity.

#### 380 **4.2 Plume pulsing behavior**

Figure 3 illustrates the temporal evolution of the Mt Bolton wildfire plume as observed by radar, highlighting a clear pulsing behavior in the vertical structure of reflectivity. Panel (a) shows a representative range–height indicator (RHI) at 03:00 UTC, where the plume exhibits a well-defined tilted structure with multiple embedded reflectivity cores. The dashed line at 6 km range marks the location at which vertical slices are extracted to construct the time–height composite shown in panel (b). At  
385 this range, the plume is sufficiently developed while remaining close enough to the radar to minimize beam broadening and sampling limitations.

The time–height composite (Fig. 3b) reveals a sequence of intermittent vertical surges in reflectivity, indicative of pulsating updraft activity within the plume. These pulses are characterized by rapid increases in reflectivity intensity and vertical



extent, followed by decay phases where both the magnitude and height of the signal decrease. The strongest pulses reach  
390 heights of approximately 2–2.5 km above ground level, with peak reflectivity exceeding 25–30 dBZ, suggesting periods of  
enhanced lofting of pyrometeors. Between these pulses, the plume exhibits a more stratified and weaker reflectivity  
structure, consistent with reduced vertical transport.

The temporal spacing of these pulses is on the order of several minutes, pointing to a quasi-periodic behavior likely driven  
by fluctuations in fire intensity and/or local atmospheric instability. Notably, the onset of stronger pulses is often preceded  
395 by a gradual buildup in low-level reflectivity, followed by a rapid vertical extension, consistent with convective-like burst  
dynamics. Occasional isolated higher-altitude echoes (e.g., around 04:28 UTC) further suggest transient injections of  
material into elevated layers, possibly associated with localized intensification or interactions with ambient wind shear.

Overall, this analysis demonstrates that wildfire plumes can exhibit pronounced pulsing behavior, with implications for  
vertical transport efficiency, plume growth, and the potential transition toward pyroconvective regimes. The use of fixed-  
400 range time–height composites provides a robust framework to quantify these dynamics and compare pulse characteristics  
across events. The full temporal evolution is provided as an animated sequence in the Supplementary Material.

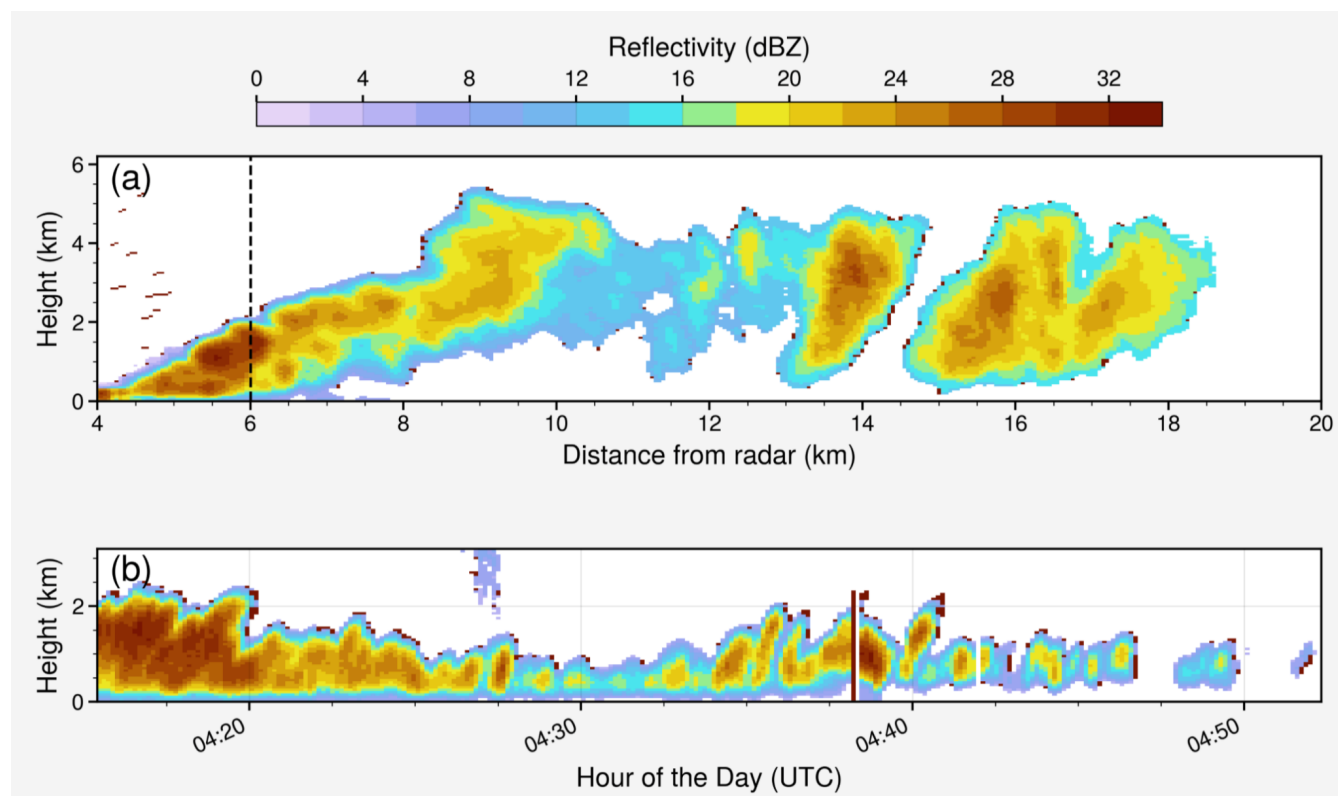
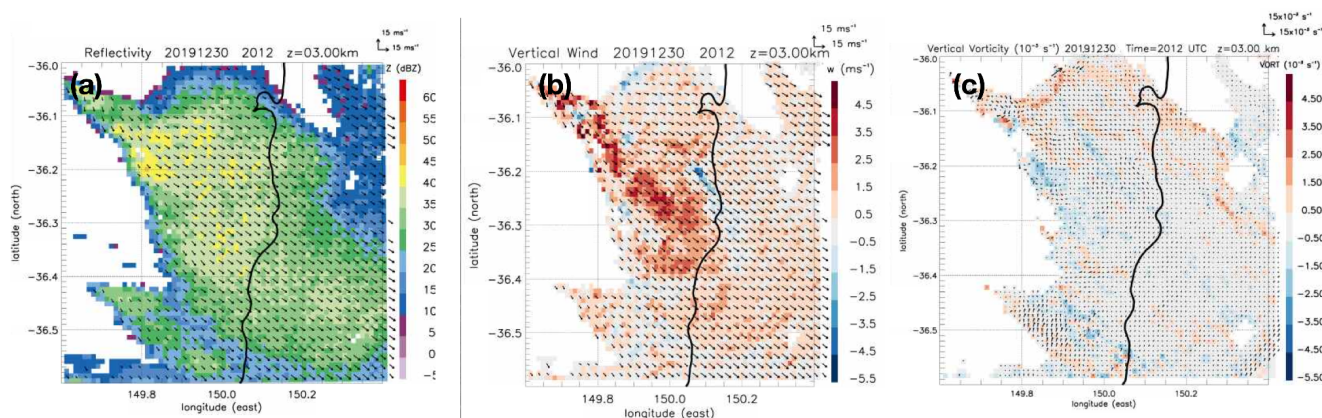




**Figure 3.** For the Mt Bolton wildfire (McCarthy et al., 2018): (a) RHI of Horizontal reflectivity [dBZ] for timestamp 04:12 UTC with dash line indicating range of 6 km from radar location, at which slices of reflectivity are extracted to construct  
 405 timeline of subpanel (b) composite timeline of vertical slices of reflectivity [dBZ] at range 6 km for the duration of the radar timeseries.

### 4.3 Kinematic signatures of extreme pyro-convection

410 The three-dimensional wind fields shown in Fig. 4 are derived from single-Doppler radar observations using a combination of Doppler velocity constraints and feature-tracking techniques (Protat et al., 2024). Because a single radar measures only the radial component of the wind, additional information is required to reconstruct the full flow field. In this study, horizontal motion is first estimated by applying optical flow to successive radar reflectivity images, which provides the advection of coherent plume features. These motion estimates are then combined with the measured radial velocities to  
 415 retrieve the horizontal wind components, while vertical velocity is obtained through continuity constraints. This hybrid approach has been shown to provide realistic convective-scale wind fields from single-Doppler observations, particularly in strongly structured flows such as pyro-convective plumes.



420 **Figure 4.** Example of wind retrievals from the Cooma wildfire in NSW on the 30 December 2019 (from the Captains Flat operational doppler radar): (a) horizontal reflectivity [dBZ] with horizontal wind vectors ( $u, v$ ) [m/s]; (b) vertical wind  $w$  [m/s] with with horizontal wind vectors ( $u, v$ ) [m/s]; (c) vertical vorticity ( $s^{-1}$ ).

Beyond plume depth and reflectivity alone, weather radar can provide physically interpretable diagnostics of the internal  
 425 dynamical organisation of pyro-convective plumes. Figure 4 illustrates this using the Cooma wildfire case in NSW during



the 2019-2020 Black Summer wildfires, where optical-flow retrievals applied to successive radar images reveal the horizontal motion field together with derived quantities including vertical velocity and vertical vorticity. The reflectivity field (Fig. 4a) shows a vertically coherent plume with enhanced echo intensity in the core, while the derived vertical-velocity field (Fig. 4b) highlights concentrated ascent embedded within the broader plume structure. The corresponding vorticity field (Fig. 4c) indicates organised rotational signatures within the convective column, demonstrating that the plume was not simply a passive smoke column but a dynamically structured fire-atmosphere circulation.

These diagnostics are consistent with previous mobile-radar and lidar observations showing that intense pyro-convective plumes can develop strong updraft cores, plume-scale rotation, and pulsing behaviour as plume elements merge and deepen. In particular, Lareau et al. (2024) documented a strongly rotating pyroCu-topped plume with a central updraft of about 35 m s<sup>-1</sup>, flanked by downdrafts, and showed that rotation intensified as discrete plume elements interacted and the plume deepened toward cloud formation. The example in Fig. 4 points to similar classes of behaviour: radar-derived flow fields can identify where ascent is concentrated, whether the plume is becoming dynamically organised, and whether rotational features are emerging within the column.

From a wildfire-intelligence perspective, this is important because these quantities move radar interpretation beyond simple plume detection toward diagnosis of how the plume is evolving. A plume that becomes narrower, more vertically coherent, and associated with stronger ascent and coherent vorticity is more likely to indicate intensified fire-atmosphere coupling than a broad but weakly organised smoke plume. Such diagnostics are therefore relevant to escalation monitoring, as they provide observational evidence of plume deepening, dynamical concentration, and the possible onset of more hazardous pyro-convective behaviour. While the present analysis remains exploratory and case-based, it demonstrates that mobile radar can resolve dynamical signatures that are directly relevant to fire behaviour and are not accessible from conventional surface observations or broad-scale satellite imagery alone.

#### 4.4 Wind change detection at low levels

Low-level wind changes represent one of the most critical hazards for fireground operations, as they can rapidly alter fire spread direction, intensity, and firefighter safety. Weather radar — including mobile X-band systems — provides a unique capability to detect these changes through clear-air echoes, Doppler velocity signatures, and boundary-layer convergence structures. Even in the absence of precipitation, refractive-index gradients, insects, ash, and fine debris can produce detectable radar returns, allowing wind boundaries and density currents to be tracked in real time (McGowan et al., 2025).

**Clear-air echoes and boundary identification.** Clear-air radar signatures have long been used to monitor mesoscale boundaries such as cold fronts, troughs, sea-breezes, and drylines. At X-band and C-band wavelengths, weak backscatter from biological targets and aerosol gradients frequently outlines convergence lines and shallow density currents. These



echoes often appear as narrow reflectivity bands accompanied by sharp Doppler velocity gradients, providing early evidence of evolving air-mass changes.

Recent work has highlighted how Doppler radar can resolve shallow boundary-layer circulations and frontal structures with depths of only a few hundred metres, enabling detailed monitoring of wind shifts relevant to fire behaviour. Such shallow features are particularly important in wildfire environments, where changes in near-surface wind direction rather than deep convection often drive rapid fire escalation.

**Convergence boundaries and gust fronts.** Mobile radar deployments have demonstrated the ability to detect convergence zones associated with thunderstorm outflows and dry gust fronts. These boundaries typically manifest as fine-line reflectivity signatures with strong radial velocity shear and, in some cases, enhanced spectrum width due to turbulence.

An example is provided by McGowan et al. (2025), in which a line of dry thunderstorms passed over an active fireground. The UQ-XPOL solid-state X-band radar captured the approaching outflow boundary in clear air ahead of the storms, revealing wind gusts up to  $25 \text{ m s}^{-1}$ . The early detection of this outflow line illustrates the operational value of mobile radar for identifying hazardous wind shifts before their arrival at the surface and impact of wildfires.

**Operational example: Southerly cool change during the 2019–2020 Australian fires.** To further demonstrate the capability of Doppler radar for detecting low-level air-mass transitions, we consider an operational case observed by the Terrey Hills radar (Sydney) during the Australian Black Summer wildfires. Although acquired with a fixed operational radar rather than a mobile system, the proximity of the instrument to the wildfires and its high sensitivity make the observations representative of what could be achieved with mobile deployments.

On 21 December 2019, extremely hot and dry north-westerly winds preceded a vigorous southerly cool change that crossed the Sydney region in the late afternoon following the passage of a trough. The wind change produced coastal gusts approaching  $100 \text{ km h}^{-1}$  at Wattamolla, approximately 20 km south of Sydney. Radar data show that the leading edge of the change formed a shallow density current roughly 500 m deep, with a well-defined radial velocity signature and a sequence of wave-like perturbations along the frontal boundary, consistent with gravity-wave activity.

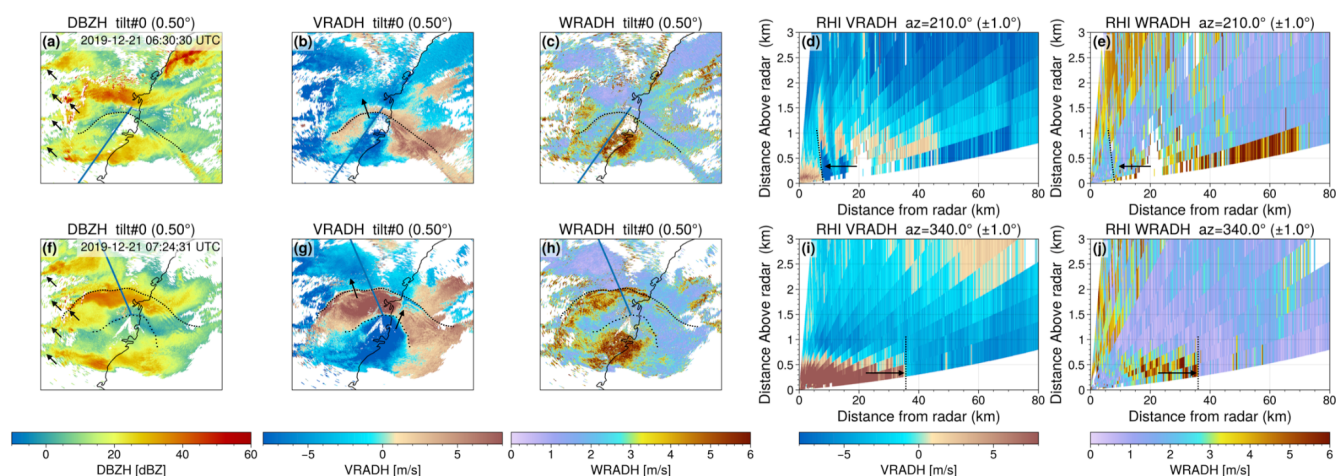
Numerous active fires were located east of the radar along the coastline at the time. The frontal structure was particularly evident in Doppler velocity (VRADH), where a sharp transition from inbound to outbound flow clearly delineated the advancing southerly surge. The radar depiction of the boundary suggests that ground crews could have received on the order of one hour of lead time prior to the arrival of the wind change, highlighting the operational relevance of clear-air Doppler observations for firefighter situational awareness.



485 **Implications for fireground monitoring.** Together, these examples demonstrate that weather radar — whether mobile or operational — can play a key role in identifying low-level wind changes that are otherwise difficult to observe over complex terrain or remote firegrounds. The ability to detect clear-air convergence lines, gust fronts, and shallow frontal boundaries provides:

- early warning of hazardous wind shifts,
- insight into boundary-layer dynamics affecting fire spread, and
- 490 • complementary information to surface observations and numerical forecasts.

When integrated with fire-agency workflows, radar-based detection of wind boundaries has the potential to substantially improve operational safety and decision-making during extreme fire events.



495 **Figure 5.** Example of frontal air masses in the lower levels captured by weather radar (Sydney (Terrey Hills) on the 21<sup>st</sup> of December 2019). Displayed are: (a) Horizontal reflectivity (dBZ) 0.5 degree tilt PPI; (b) radial velocity (m/s) 0.5-degree tilt PPI; (c) spectrum width (m/s) 0.5-degree tilt PPI; (d) pseudo-RHI along azimuth 210 degrees for timestep of the first row of subpanels for radial velocity; (e) pseudo-RHI for spectrum width.

#### 4.5 Indicators of pyroCu to pyroCb escalation

500 The transition from pyro-cumulus (pyroCu) to pyro-cumulonimbus (pyroCb) represents a critical stage in extreme fire-atmosphere coupling, as it marks the onset of deep convection, ice-phase microphysics, and potentially hazardous outflows. Previous studies (e.g. Terrasson et al., 2019; McCarthy et al., 2023) highlight that radar observations can document this



escalation through rapid plume deepening, echo intensification, and distinct temporal evolution. Here, we discuss these indicators from an exploratory perspective, without implying predictive capability.

To illustrate how weather radar can quantify the growth of pyroconvective clouds and provide intelligence on precipitation type, dynamics, and potential hazards, we examine a case observed during the Australian Black Summer wildfires using an operational weather radar located approximately 100 km from the fireground. Although the distance reduces sensitivity to fine-scale structures, the magnitude of the developing pyroCb produced strong echoes, offering insight into what a mobile radar might resolve at closer range.

Figure 4 documents the evolution of one of the pyroconvective clouds associated with the Gosper fire. At 02:40 UTC, a vertically developed smoke column topped by a pyroCu reached approximately 8 km above sea level. Conventional hydrometeor classification (CSU) misidentified the scattering signatures, labelling them as drizzle, wet snow, or aggregates (Fig. 4c1). Visual observations and previous studies indicate that below the condensation level the plume consisted predominantly of pyrometeors, while above this level a mixture of small droplets and abundant ash particles dominated the scattering (McCarthy et al., 2019; Lareau et al., 2024). Texture-based methods (Guyot et al., 2023) successfully detected the smoke plume at lower tilts but were not applicable here to higher elevations or to detailed hydrometeor classification.

By 03:00 UTC the cloud had transitioned to a pyroCb, exceeding 12 km in altitude and developing an anvil structure with ice crystals extending near or above the tropopause. The presence of graupel inferred from polarimetric signatures is consistent with previous modelling and observational studies of pyroCb microphysics (Rosenfeld et al., 2007; Couto et al., 2024). Enhanced radial Doppler velocities observed at upper levels (Fig. 4b2) suggest strong updrafts supporting rapid vertical growth. One hour later, at 04:00 UTC, the storm top reached approximately 14 km, with hail signatures emerging within the cloud (Fig. 4c3). Concurrently, Doppler velocity patterns indicated the development of rotational structure, highlighting the increasing dynamical complexity of the fire-triggered thunderstorm.

These observations emphasize several exploratory indicators of escalation from pyroCu to pyroCb:

- **Rapid plume deepening**, reflected by increasing echo tops and vertical growth rates.
- **Echo intensification**, associated with the onset of ice-phase processes and graupel or hail formation.
- **Temporal thresholds**, where structural changes occur on timescales of tens of minutes to an hour rather than gradual evolution.

While such signatures demonstrate the capability of weather radar to document pyroconvective escalation, they should be interpreted as diagnostic rather than predictive indicators. Further work combining radar observations, numerical modelling, and multi-sensor datasets will be required to establish robust operational thresholds.

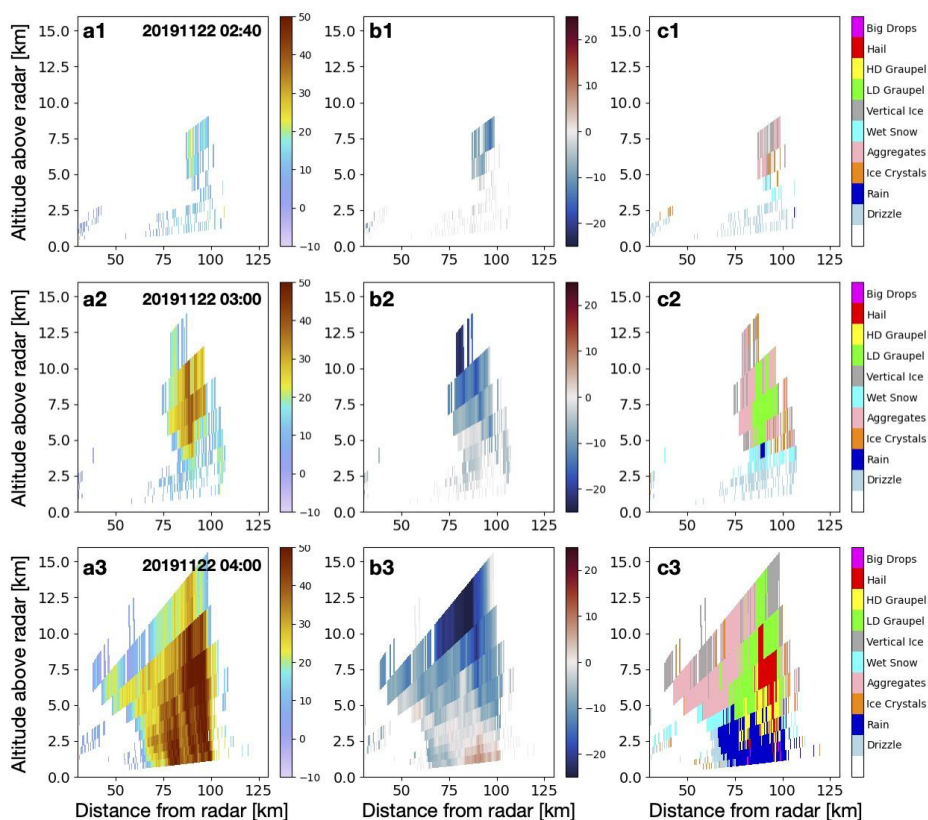


**Figure 6.** Range Height Indicator (RHI) from the Terrey Hills radar on the 22<sup>d</sup> of November 2019, at the azimuth 320 degrees to the North, capturing the radar signatures of a forming pyroCb.

535

#### 4.6 Firebrand identification and tracking

Identification and tracking of firebrands, e.g. burning debris capable of initiating spot fires beyond the main flame front, remain major challenges in wildfire monitoring and prediction due to their small size, complex transport, and critical role in rapid fire spread. Two complementary approaches from recent literature demonstrate progress in both observational  
540 detection and predictive modelling of firebrand behaviour.



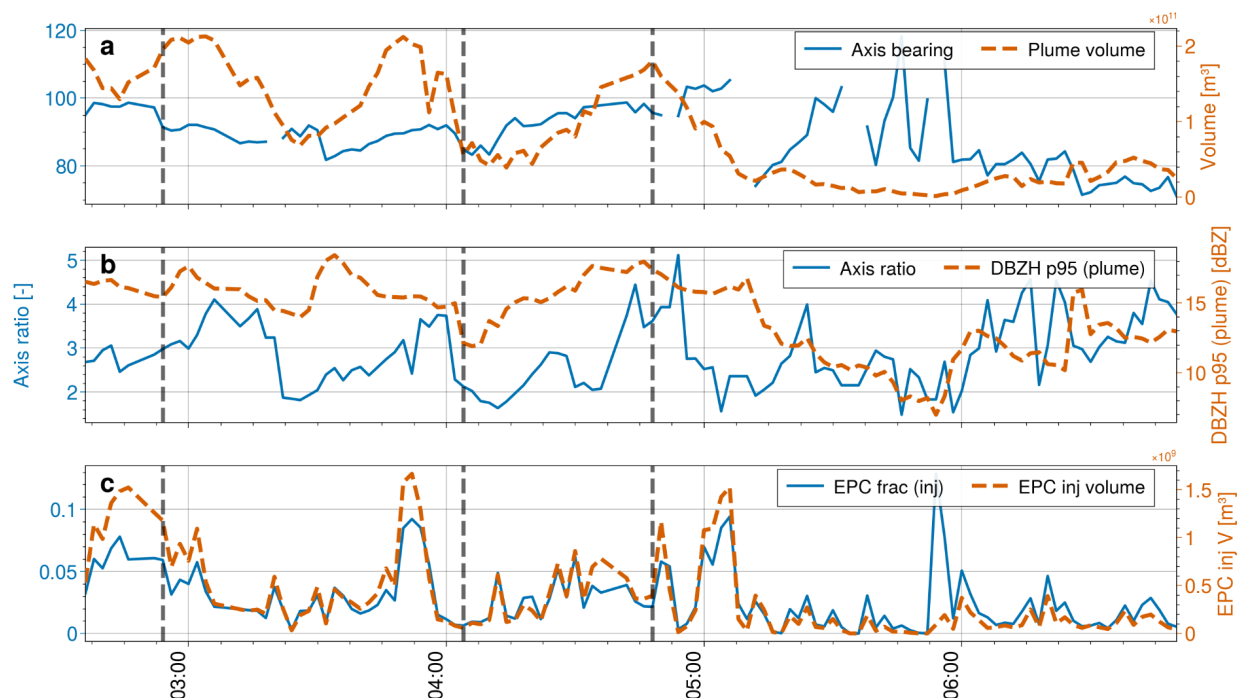
McCarthy et al. (2019) developed a novel observational framework using dual-polarised X-band weather radar coupled with an unsupervised machine learning classifier (Gaussian Mixture Model) to distinguish between different pyrometeor classes in wildfire plumes, including firebrands. In this work, “pyrometeors” are defined as large biomass combustion debris lofted into the atmosphere (>2 mm) that produce distinct polarimetric radar signatures. The classification isolates coherent radar features most likely associated with firebrands, enabling their tracking in time and space through successive radar scans. This method demonstrates that wildfires produce detectable radar returns from firebrands and that their spatiotemporal evolution can be monitored, potentially supporting spot-fire risk assessment and improving situational awareness during active wildfires.

## 5. Demonstration case study: integrated analysis

Having established the diagnostic framework above, and to illustrate the operational and scientific value of weather radar for documenting extreme wildfire behaviour, we draw on a recent case study of the Wallangarra wildfire (31 October 2023) in southeast Queensland, Australia, previously analysed in detail by McGowan et al. (2026). In that study, a mobile X-band polarimetric Doppler radar (UQ-XPOL) was deployed in complex terrain and captured multiple transitions between wind-driven and plume-driven fire behaviour, including explosive pyroCu development, pyrometeor lofting, and episodic plume pulses. Here, rather than re-examining the full meteorological evolution, we use this event specifically to demonstrate how radar observations can quantify plume growth, characterise scatterer properties, identify pyrometeor transport linked to spotting, and diagnose dynamical signatures associated with pyroconvective escalation. The dataset and methods are presented in Supplementary material together with associated figures S1 and S2.

### 5.1 Chronology of the events with plume metrics

Figures 7–10 demonstrate that weather radar resolves not only the geometric evolution of the plume but also key physical mechanisms governing pyroconvective development and particle injection.



565

**Figure 7.** Time series (time in UTC) of variables derived from plume properties: (a) axis bearing to the geographic north and plume volume [m<sup>3</sup>]; (b) axis ratio derived from PCA and 95<sup>th</sup> percentile of DBZH [dBZ]; (c) EPC fraction within injection zone and EPC injection volume [m<sup>3</sup>].

The time series in Figure 7 show well-defined high intensity peaks (at 3:00, 3:50 and 4:50 UTC) during which plume volume, axis ratio, high-percentile reflectivity (95<sup>th</sup> percentile DBZH) (to a lesser extent), and Enhanced Pyrometeor Cluster (EPC) activity increase simultaneously. The growth in plume volume reflects enhanced vertical transport and mass loading, while the increase in the PCA-derived axis ratio indicates sustained alignment with the ambient flow, consistent with a mature, momentum-driven plume. The concurrent rise in 95<sup>th</sup> percentile DBZH points to an increase in the concentration and/or effective size of radar-resolved scatterers within the plume core.

Most notably, the EPC fraction and EPC injection volume within the defined injection cuboid increase sharply during the peak phase. Given that EPCs are characterised by elevated reflectivity and enhanced differential signatures, their amplification is consistent with intensified lofting of larger or more numerous particles. This behaviour supports a mechanism in which stronger updrafts promote the vertical transport of coarse ash aggregates and/or firebrands, potentially accompanied by aggregation processes within the turbulent core. The tight temporal coupling between plume elongation, reflectivity enhancement, and EPC injection suggests that particle production and plume dynamics are directly linked rather than independently varying.

580

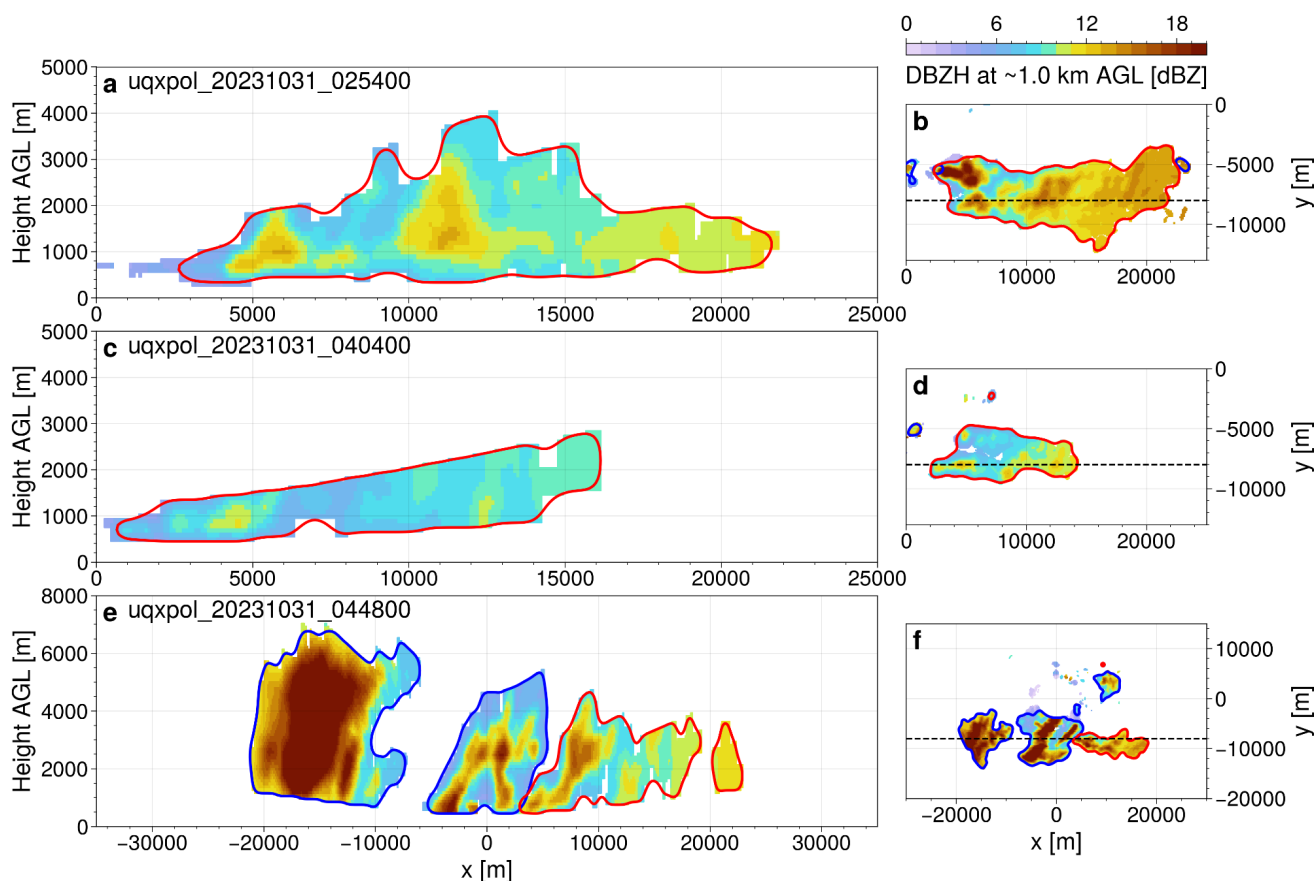


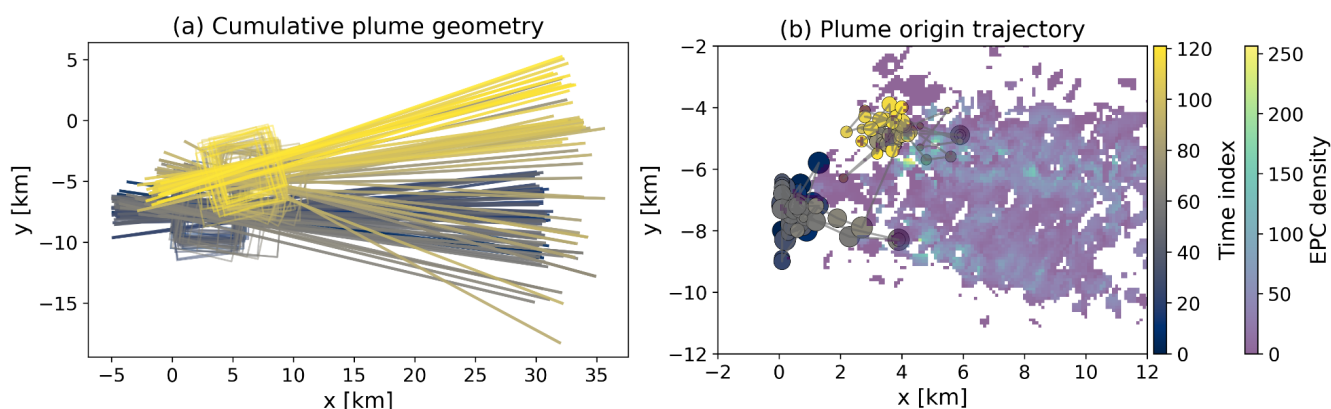
**Figure 8. (a-f)** RHI and horizontal slices at 1 km elevation above ground level of DBZH [dBZ] taken at three chosen timestamps (in UTC) as indicated by vertical dashed lines in figure 7.

585 The vertical (Figure 8a,c,e) and horizontal (Figure 8b,d,f) snapshots confirm this interpretation. During the intense phase, cross sections reveal rapid vertical growth and the emergence of vertically coherent high-DBZH cores, characteristic of strengthened convective updrafts (Figure 8a, b). During lower intensity phases (Figure c,d) reflectivity remains vertically confined, indicative of limited buoyant forcing. Simultaneously, horizontal slices at 1 km AGL show increased spatial coherence and elongation, consistent with sustained momentum transport. At peak activity, the plume exhibits maximum depth and the most pronounced reflectivity gradients, aligning with the maxima in EPC fraction and injection volume. These structural changes demonstrate the radar’s ability to directly resolve the transition from a weakly buoyant smoke column to a dynamically organised pyroconvective system. In Figure 8e,f, the air mass change bringing precipitating clouds are seen approaching the fireground (blue contours) and interacting with the fire plume (red contours). The radar polarimetric data shows precipitation as the shape of droplets elongate (Figure S2).

590

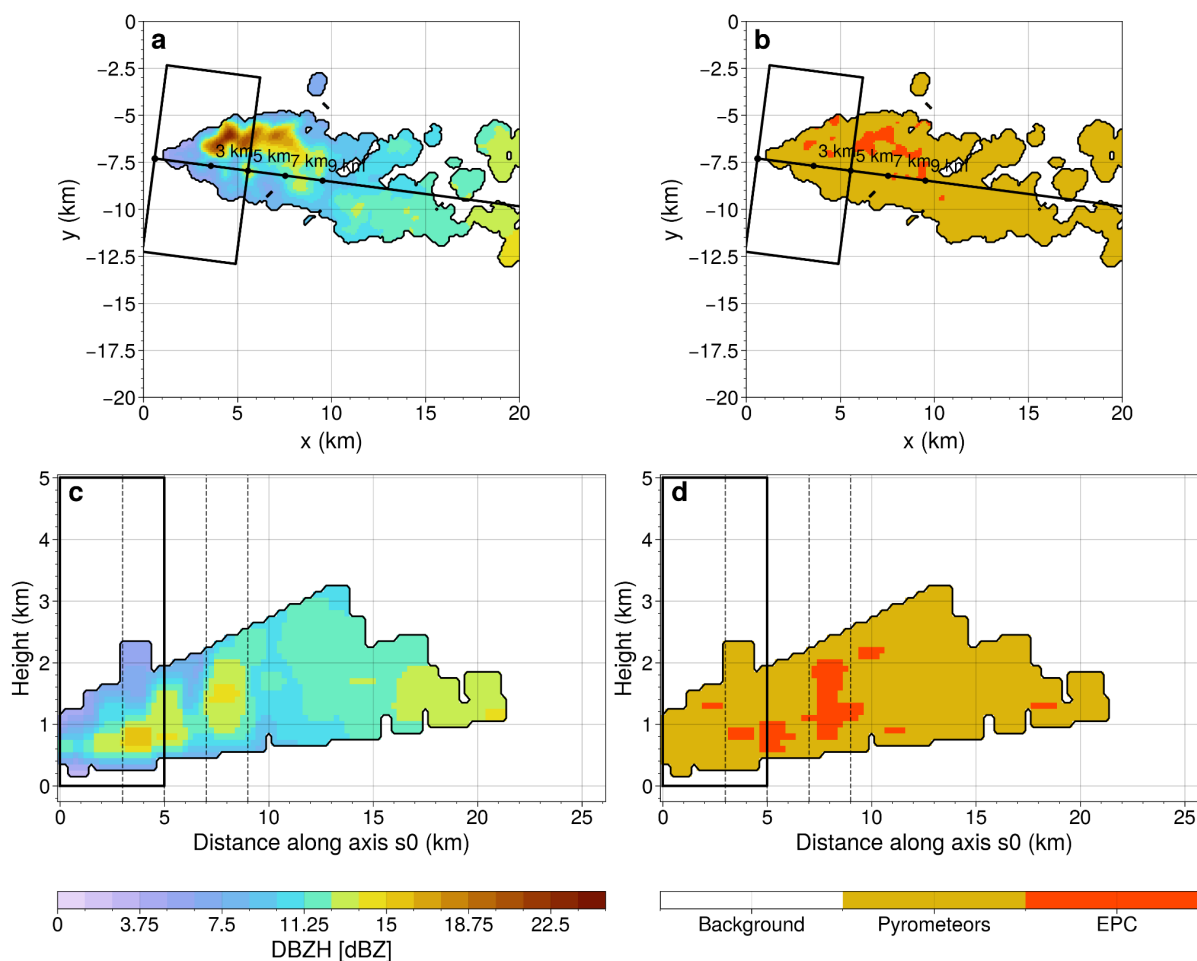


595 Time-integrated diagnostics (Figure 9) further highlight the persistence of the dominant transport axis and a spatially coherent injection region. The progression of plume origins, scaled by injected volume and EPC density and coloured by time, reveals the two different periods captured by the radar: the first phase (in grey) with large injection volumes (large circles) and West-East main axis and second phase with much reduced intensity after the passage of the air mass (McGowan et al., 2026) and a plume oriented further to the East-North-East. The clustering of large, high-density markers during the peak period indicates that enhanced particle injection is spatially focused near the source and temporally associated with the most vigorous convective phases. This pattern is consistent with episodic bursts of fire-driven updraft strengthening rather than continuous low-level emission.



605 **Figure 9.** Plume average properties over the full period: (a) main axis and location of defined injection cuboid; (b) plume origin where size of circles are proportional to the injected volume and Enhanced Pyrometeors Clusters (EPC) density. The grey-to-yellow colour code indicates time (normalised).

The detailed view at 02:42 UTC (Figure 10) illustrates these mechanisms at maximum activity. The horizontal slice at 1 km AGL shows a strongly elongated high-reflectivity core aligned with the principal axis. Segmentation highlights EPCs concentrated within this core but extending to up to 8 km within the plume. Cross sections extracted along the main axis reveal vertically coherent reflectivity maxima co-located with EPC-rich regions, indicating that enhanced particle populations are embedded within the primary updraft pathway. The confinement of maximum EPC density and injection volume to a limited downwind distance from the origin supports the hypothesis of focused, high-energy lofting capable of transporting larger particles before gravitational settling dominates.



615 **Figure 10.** Horizontal slide of (a) DBZH [dBZ] at 1km above ground level and (b) segmented pyrometeors highlighting in red the Enhanced Pyrometeors Clusters; cross sections taken along the axis s0 as shown in (a) and (b) of DBZH [dBZ] and the classification. Origin of the plume and distance from origin are also shown along the s0 axis. These snapshots are taken at a timestamp of 2:42 UTC at a peak of pyroconvective activity (as shown in figure 7).

Collectively, these results show that operational weather radar can resolve several key mechanisms of pyroconvection: (i) strengthening of buoyant updrafts and vertical plume growth, (ii) dynamical organisation and alignment with environmental flow, (iii) enhanced concentration and/or aggregation of larger scatterers within the plume core, and (iv) temporally concentrated bursts of particle injection consistent with intensified fire activity. The combined geometric and polarimetric diagnostics therefore provide quantitative evidence that radar observations can capture both the dynamical and microphysical signatures of extreme fire-driven convection.

620



## 625 5.2 Visualisation

To enhance operational interpretability, segmented radar echoes were rendered in three dimensions over regional topography derived from the Shuttle Radar Topography Mission (SRTM) dataset (Figure 11). This visualisation integrates classified pyrometeors and hydrometeors within their geographic and terrain context, providing a spatially intuitive representation of plume structure and evolution. The 3D view enables rapid assessment of plume depth, tilt, and spatial extent relative to the  
630 fireground and surrounding terrain. In complex landscapes, such contextualisation is critical for understanding how topography influences plume anchoring, channeling, and downwind transport pathways (McGowan et al., 2026). The separation of pyrometeor-dominated regions from hydrometeor echoes further clarifies zones of active lofting and potential pyrometeors' transport, supporting interpretation of escalation phases and interactions with approaching weather systems.

From an operational perspective, this type of visual product translates radar-derived diagnostics into a format readily usable  
635 during incident briefings and situational awareness updates. By combining terrain, plume geometry, and classification in a single view, the visualisation reduces the need for expert interpretation of multiple two-dimensional radar panels. When integrated within a real-time dashboard or multi-sensor display environment, or within a fire behavior simulator software such as Spark (Fox-Hugues et al., 2024), 3D radar products can support rapid communication between meteorologists, fire behaviour analysts, and incident controllers.

640 Although quantitative metrics remain central for objective assessment, immersive visual representations such as Figure 11 enhance comprehension of fire–atmosphere interactions and provide a practical pathway for embedding radar observations within operational wildfire intelligence workflows.

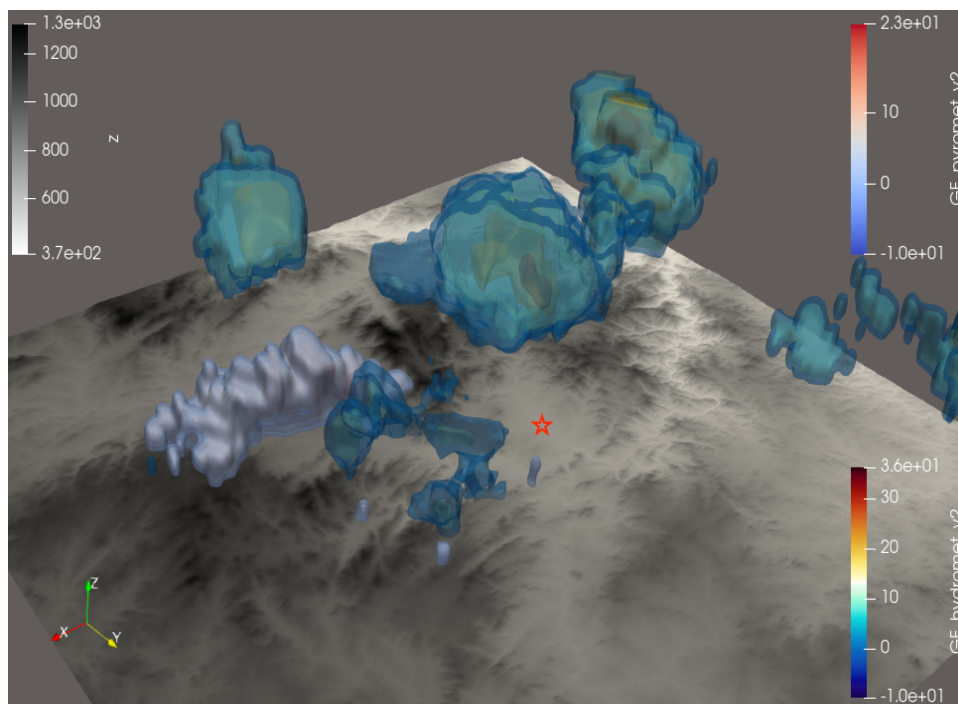


**Figure 11.** 3D visualisation of the segmented radar echoes (hydrometeors and pyrometeors) over regional topography (SRTM). The red star indicates the location of the UQ XPOL weather radar.

645

## 6. Integration with existing wildfire intelligence tools

Portable weather radar observations should be viewed as a complement rather than a replacement for existing wildfire intelligence systems. Geostationary satellite remote sensing provides high temporal resolution but coarse spatial resolution of cloud top temperatures or fire radiative power when not obstructed by clouds, while numerical models and in-situ observations offer environmental guidance. Radar uniquely bridges these scales by resolving the internal dynamics of smoke plumes and pyro-convective clouds at high spatial and temporal resolution.

650

### 6.1 Complementarity with geostationary satellites

Geostationary satellites and mobile weather radar provide complementary and scale-bridging perspectives on wildfire plumes. Satellite platforms offer continuous regional coverage and are particularly effective for monitoring cloud-top temperature, plume-top height proxies, and fire radiative power. Cloud-top brightness temperatures provide insight into convective depth and the thermodynamic phase of pyroconvective clouds, supporting identification of transitions from

655



pyroCu to deep, ice-phase pyroCb. However, satellite observations are constrained by spatial resolution (typically ~ 2 km at nadir in thermal bands) and temporal sampling (~ 2.5–10 minutes depending on scan mode), limiting their ability to resolve  
660 rapid internal structural changes and sub-kilometre plume dynamics. In addition, parallax effects inherent to geostationary viewing geometry can horizontally displace elevated cloud features, complicating direct spatial comparison with ground-based observations, particularly during deep convective development.

Mobile weather radar, deployed closer to the fireground, resolves the three-dimensional internal structure of the plume at typically 100 m resolution and minute-scale updates. It captures vertical growth, embedded updraft cores, particle  
665 concentration changes, and low-level wind interactions that are not directly observable from space. Because mobile radar can provide accurate plume height and geometric structure, it also offers a reference framework for parallax correction and improved satellite–radar co-registration during integrated analyses.

Together, satellite observations provide the large-scale convective context and cloud-top evolution, while mobile radar resolves the internal dynamical and microphysical processes driving escalation. Their combined use enables a physically  
670 consistent, multiscale characterisation of fire–atmosphere interactions and strengthens the observational basis of wildfire intelligence systems.

## 6.2 Integration with fire behaviour models

Coupled fire-atmosphere models have been used in the last 30 years to describe the interactions between fires and the  
675 atmosphere while accounting for detailed topography and fuel description (Clark et al., 1996; Skamarock et al., 2006; Kochanski et al., 2011; Filippi et al. 2018; Peace et al. 2016). To verify these models, highly instrumented grass fires such as the Fireflux I experimental campaign conducted by Clements et al. (2007) have been used (Kochanski et al., 2013; Filippi et al., 2013). Although these campaigns are useful to analyse how well the models reproduce the atmospheric interactions near the ground and dynamic events during the fire front passage, they can not be scaled to large wildfires with a well-developed  
680 or convective plume.

Portable weather radar can then be used as a model evaluation tool to determine the ability of these models to describe large wildfire events. The first type of model evaluation metrics can be related to slowly changing metrics such as the plume top height and plume bottom height, plume depth and the plume shape. Indeed, most coupled fire-atmosphere models inject a passive tracer that is usually considered as smoke allowing to derive the just mentioned metrics (Baggio et  
685 al., 2022).

Secondly, due to their high frequency sampling rate, portable radar can also be used to describe the plume dynamics. We refer here for example the shifts in wind direction and intensity directly affecting the plume shape, the horizontal main axis for well-developed plumes, and dynamic changes in the plume height that could be linked to a more



intense fire. Coupled fire-atmosphere can also provide high frequency (~ seconds) 3D fields or directly calculating the above  
690 mentioned fields during the timestep.

Finally, the LES models used in the coupled fire-atmosphere models usually describe well the hydrometeor  
dynamics, which can also be observed by mobile radar (McCarthy et al., 2018; Alonso-Pinar et al., 2026). More recently,  
pyrometeor (ashes, firebrands as described in McCarthy et al. (2020)) observations from radar measurements have been used  
to verify firebrand trajectories using both Lagrangian (Sun et al., 2026) and Eulerian formulations (Alonso-Pinar et al.,  
695 2026). Portable radar measurements can be directly used to verify, validate and improve radar forward operators in LES  
models. However, radar operators only reproduce the hydrometeors echoes and none has been developed for pyrometeors.

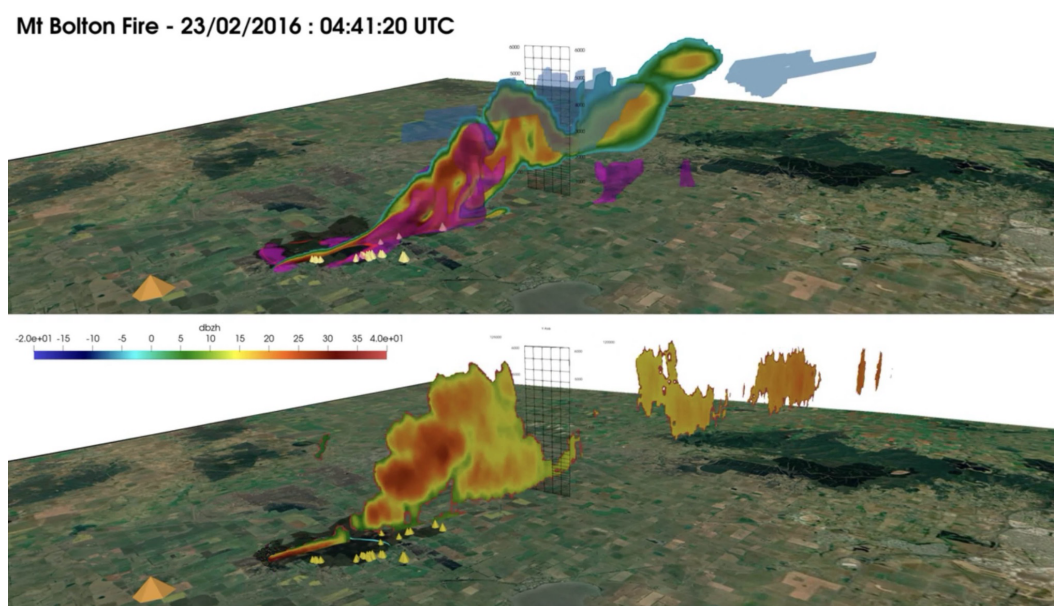


**Figure 12.** Comparison between coupled fire-atmosphere simulation and mobile radar observations for the Mt Bolton  
700 (McCarthy et al., 2018) wildfire.

The comparison is shown at 04:01:20 UTC. In the top panel, the passive smoke tracer is shown in orange, with darker shades  
indicating higher concentration. The purple isovolume shows significant spotting mass concentration, which, unlike the  
passive tracer, is subject to sedimentation. The blue isosurface indicates regions where the liquid water ratio exceeds 0, i.e.  
where liquid water or ice is present. The weather radar location is indicated by the large orange cone on the left. The bottom  
705 panel shows the corresponding radar observation, with attenuation plotted in the same plane.



This side-by-side view is used to compare the simulated plume structure with the observed one, in terms of extent, vertical development, displacement, and internal composition. It is particularly useful for checking whether the model captures the main dynamical and microphysical features visible in the radar data.

710

### 6.3 Conceptual operational workflow

The proposed capability is designed to supplement existing wildfire incident management workflows by introducing radar-derived information that is not available from current satellite, model, or ground-based observations alone. Rather than redefining operational practices, the system integrates with established monitoring processes to enhance situational awareness during rapidly evolving fire behaviour.

715

During pre-event and early monitoring, satellite observations, numerical weather prediction, and fire intelligence remain the primary sources of situational awareness. Radar contributes opportunistically by providing additional context on plume structure and atmospheric response once active convection develops, without altering existing decision pathways.

720

In the active fire phase, radar observations, including portable deployments where appropriate, provide unique insight into the vertical structure and evolution of fire plumes, wind variability within and around the plume, and rapid transitions such as strengthening updrafts or sudden downdrafts, and early formation of pyrocumulus and escalation to pyrocumulonimbus. These measurements complement satellite imagery by resolving features that are otherwise obscured by smoke or limited by temporal resolution, enabling earlier detection of hazardous changes affecting crew safety and fire spread potential.

725

As fires escalate, multisensor integration combines radar-derived indicators with satellite products and short-term forecasts to support interpretation rather than automation. The objective is to provide incident teams with additional evidence on plume intensity, potential wind changes signatures, and evolving fire-atmosphere interactions, helping reduce uncertainty during critical decision points.

730

Following an event, archived radar and multisensor datasets support post-incident analysis, training, and refinement of operational procedures. By embedding radar-derived products within existing workflows, the approach aims to progressively demonstrate added value while minimising disruption to established practices.

## 7. Discussion and Technology Readiness Level assessment



735 The maturity of portable weather radar applications for wildfire observation and intelligence can be assessed using the Technology Readiness Level (TRL) framework (Mankins, 1995), which provides a structured pathway from fundamental research to operational deployment. While weather radar hardware is itself fully mature within meteorological applications, its specific use for wildfire intelligence represents a distinct technological and operational capability that remains under development.

740 At present, the interpretation of radar signatures from wildfire plumes is constrained by limited understanding of the scattering properties of pyrometeors, including ash, embers, and mixed-phase particles. This aspect of the problem remains at low TRL (2–3), where physical principles are established but robust, frequency-dependent scattering models and retrieval algorithms have yet to be validated. Progress in this area is essential to enable quantitative interpretation of radar reflectivity and polarimetric variables across radar bands.

**Table 2.** Technology Readiness Level (TRL) assessment for portable weather radar applications in wildfire intelligence.

745

TRL	Description	Current status	Key references / examples
1–3	Fundamental principles observed and conceptualised	Scattering mechanisms of ashes, firebrands, and mixed pyrometeors remain poorly constrained. Polarimetric interpretation is largely empirical and frequency-dependent.	Rogers et al. (1997); McCarthy et al. (2018, 2019); Kingsmill et al. (2023); Lareau et al. (2024); analogy to hail scattering (Mirkovic et al. 2019, 2021). Guyot et al. (2023).
4	Technology validated in laboratory or controlled research settings	Early portable radar deployments demonstrated detectability of wildfire plumes and basic kinematic signatures in opportunistic or prescribed burn settings.	Wurman and Weygandt (2003); Palumbo et al. (2013); Palumbo (2016)
5	Technology validated in relevant environment	Dedicated field campaigns capturing wildfire plume dynamics, polarimetric signatures, and updraft structures at safe operational distances.	McCarthy et al. (2018, 2020); Aydell and Clements (2021); Kingsmill et al. (2023)



5-6	Prototype system demonstrated in relevant environment	Emerging radar-derived diagnostics such as plume depth evolution, wind change detection in clear air, and pyro-convective lifecycle monitoring. Validation remains limited to a small number of case studies.	McCarthy et al. (2023); May et al. (2024); Lareau et al. (2024); McGowan et al (2025, 2026).
6	System/subsystem demonstrated in operationally relevant context	Conceptual integration of portable radar within wildfire intelligence frameworks, including deployment protocols, safety constraints, and coordination with incident management.	This study; proposed framework
7-9	Operational system proven and routinely used	Not yet achieved. Requires standardised procedures, trained personnel, automated products, and integration with existing agency tools.	

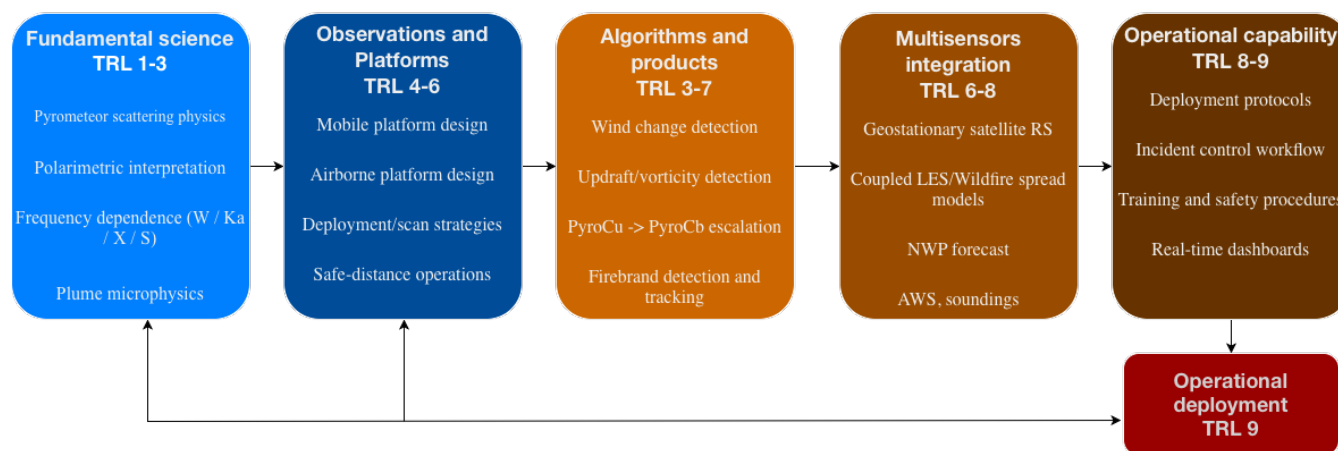
750 Portable radar deployments observing wildfires and prescribed burns have reached TRL 4–5, demonstrating feasibility and repeatability in relevant operational environments. Multiple studies have shown that mobile X-, Ka-, and W-Band radars can be safely deployed at appropriate distances from active fires on the ground and in aircraft, and can capture key dynamical features of pyro-convective plumes, including updrafts, rotation, and plume growth. These deployments provide strong evidence that the technology is sufficiently mature for sustained research use and for the development of prototype applications.

755 Emerging radar-derived products, such as wind change detection in clear-air conditions and diagnostics of plume deepening and convective escalation, currently sit near TRL 4–5. While these capabilities have been demonstrated in a limited number of case studies, broader validation across diverse fire regimes and atmospheric conditions is required before they can progress toward TRL 6. Such advancement will depend on expanded observational datasets and the development of automated, robust algorithms suitable for near-real-time use.

The transition to TRL 6 and beyond will be driven less by further advances in radar hardware than by organisational, algorithmic, and integration challenges. These include the establishment of operational deployment protocols, training



760 pathways within fire agencies, integration with satellite-based wildfire monitoring systems, and the incorporation of radar-derived products into existing decision-support frameworks. Achieving these steps would mark the progression from experimental research capability to pre-operational wildfire intelligence, paving the way toward routine operational use in the longer term.



765 **Figure 13.** Conceptual roadmap illustrating the progression from fundamental radar science to operational wildfire intelligence. The diagram highlights the central role of algorithm development and multi-sensor integration in advancing portable weather radar applications toward higher Technology Readiness Levels (TRL). Arrows indicate the transition from research to operational capability, while the feedback pathway emphasises the role of field deployments in driving continued scientific advancement.

770 **8. Conclusion**

Extreme wildfire behaviour is driven by tightly coupled fire–atmosphere processes that evolve on spatial and temporal scales not fully resolved by existing monitoring systems. This study synthesised two decades of portable radar deployments and presented new analysis from a recent mobile X-band radar observation of an extreme wildfire in Eastern Australia to evaluate the role of weather radar within wildfire intelligence.

775 We demonstrate that portable weather radar can resolve key mechanisms of pyro-convection, including plume deepening, dynamical organisation and alignment with environmental flow, wind boundary interactions, and temporally concentrated pyrometeors’ injection. In the Wallangarra case study, radar-derived diagnostics quantified plume geometry, axis stability and origin, and the evolution of Enhanced Pyrometeor Clusters (EPC), providing observational evidence of intensified



780 lofting and focused injection during peak fire activity. These results show that radar observations can move beyond qualitative plume detection toward physically interpretable metrics directly linked to fire behaviour escalation.

Radar complements existing intelligence tools by bridging the scale gap between satellite remote sensing, numerical modelling, and sparse surface observations. While satellites provide regional cloud-top and radiative signatures, mobile radar platforms resolve the internal structure, vertical growth, and low-level dynamical evolution of wildfire plumes at high spatial and temporal resolution. In complex terrain and rapidly evolving firegrounds, this provides access to plume dynamics and hazardous transitions that are not captured by existing operational observing systems.

785 Within a Technology Readiness Level (TRL) framework, portable radar deployments have reached intermediate maturity (TRL 4–5), with repeated demonstrations in relevant wildfire environments. Emerging radar-derived products approach pre-operational capability. The principal challenges to higher readiness are no longer hardware limitations, but improved understanding of pyrometeor scattering, algorithm robustness, automated product generation, and institutional integration within fire agency workflows.

Beyond real-time situational awareness, portable weather radar also offers strong potential as a post-incident analysis and model evaluation tool. Comparisons between radar-derived plume structure, dynamics, and particle injection signatures and coupled fire–atmosphere simulations can help identify where models reproduce, or fail to reproduce, key transitions in fire behaviour associated with topography, wind forcing, and fire–atmosphere coupling. In this way, radar observations contribute both to improved physical understanding and to the refinement of predictive modelling frameworks used to support fire behaviour analysis and operational planning. Advancing portable radar toward operational wildfire intelligence will require systematic multi-event validation, multisensor integration, and the development of clear, standardized products tailored to fire agency workflows. With these steps, portable weather radar has the potential to become a valuable operational asset, strengthening situational awareness, enabling more informed resource allocation, and improving decision-making during extreme wildfire events.

### **Code and data availability**

795 The code was developed at The University of Queensland, at The Australian Bureau of Meteorology and during AG’s free time in January to March 2026. The software to produce products from XPOL remains the intellectual property of the author and is not currently available in the public domain. The code is not available in the public domain. UQ XPOL data is available at <https://zenodo.org/records/13743539> [last accessed 9 October 2024].



### Author contributions

AG designed the concept of the paper with feedback from all co-authors. Original datasets were collected by several people and are cited in the references of this article. AG analysed the data and created the figures and diagrams. All co-authors provided regular scientific inputs. AG prepared the original manuscript with contributions from all co-authors.

### 810 Competing interests

Dr Jean-Baptiste Filippi is a member of the editorial board of EGU-NHESS. The contact author declares that here is no other competing interests for himself or other co-authors.

### Acknowledgements

815 This project was undertaken with the assistance of resources from the Australian National Computational Infrastructure (NCI) and the Australian Bureau of Meteorology, both of which are supported by the Australian Government. Thanks to Laura Carrascosa (formally at University of Queensland Enterprise Research Partnership) for introducing the TRL concept to the first author of this paper. AI tools (Large Language Models) have been used to improve wording, check grammar and punctuation of the manuscript.

### Financial support

820 This research was directly supported by *Google.org*, the non-profitable branch of Google (Grant TF2103-098173).

### References

- Abatzoglou, J. T., Kolden, C. A., Williams, A. P., Sadegh, M., Balch, J. K., and Hall, A.: Downslope wind-driven fires in the western United States, *Earth's Future*, 11, e2022EF003471, <https://doi.org/10.1029/2022EF003471>, 2023.
- 825 Alonso-Pinar, A., Filippi, J.-B., Guyot, A., McCarthy, N., Tulet, P., and Filkov, A.: Eulerian modelling of spotting using a coupled fire–atmosphere approach, *EGUsphere* [preprint], <https://doi.org/10.5194/egusphere-2025-4855>, 2025.
- Aydell, T. B. and Clements, C. B.: Mobile Ka-band polarimetric Doppler radar observations of wildfire smoke plumes, *Mon. Weather Rev.*, 149, 1247–1264, 2021.



- Banta, R. M., Olivier, L. D., Holloway, E. T., Kropfli, R. A., Bartram, B. W., Cupp, R. E., and Post, M. J.: Smoke-column observations from two forest fires using Doppler lidar and Doppler radar, *J. Appl. Meteorol.*, 31, 1328–1349, [https://doi.org/10.1175/1520-0450\(1992\)031<1328:SCOFTF>2.0.CO;2](https://doi.org/10.1175/1520-0450(1992)031<1328:SCOFTF>2.0.CO;2), 1992.
- 830 Baggio, R., Filippi, J.-B., Truchot, B., and Couto, F. T.: Local- to continental-scale coupled fire–atmosphere simulation of a large industrial fire plume, *Fire Saf. J.*, 134, 103699, <https://doi.org/10.1016/j.firesaf.2022.103699>, 2022.
- Birch, R. L.: Radar observations of smoke, *Aust. Meteorol. Oceanogr. J.*, 16, 30–31, 1968.
- 835 Baum, T., Thompson, L., and Ghorbani, K.: Complex dielectric measurements of forest fire ash at X-band frequencies, *IEEE Geosci. Remote Sens. Lett.*, 8, 859–863, <https://doi.org/10.1109/LGRS.2011.2131119>, 2011.
- Baum, T. C., Thompson, L., and Ghorbani, K.: The nature of fire ash particles: microwave material properties, dynamic behavior, and temperature correlation, *IEEE J. Sel. Top. Appl. Earth Obs. Remote Sens.*, 8, 480–492, <https://doi.org/10.1109/JSTARS.2014.2386394>, 2015.
- 840 Campos, C., Couto, F. T., Santos, F. L. M., Pinto, P., Purificação, C., Silva, H. M., et al.: Assessing wildfire dynamics during a megafire in Portugal using the MesoNH/ForeFire coupled model, *Q. J. R. Meteorol. Soc.*, e70075, <https://doi.org/10.1002/qj.70075>, 2025.
- Carroll, B. J., Brewer, W. A., Strobach, E., Lareau, N., Brown, S. S., Valero, M. M., Kochanski, A., Clements, C. B., Kahn, R., Junghenn Noyes, K. T., Makowiecki, A., Holloway, M. W., Zucker, M., Clough, K., Drucker, J., Zuraski, K., Peischl, J., 845 McCarty, B., Marchbanks, R., Sandberg, S., Baidar, S., Pichugina, Y. L., Banta, R. M., Wang, S., Klofas, A., Winters, B., and Salas, T.: Measuring coupled fire–atmosphere dynamics: The California Fire Dynamics Experiment (CalFiDE), *Bull. Am. Meteorol. Soc.*, 105, E690–E708, <https://doi.org/10.1175/BAMS-D-23-0012.1>, 2024.
- Christian, K., Wang, J., Ge, C., Peterson, D., Hyer, E., Yorks, J., and McGill, M.: Radiative forcing and stratospheric warming of pyrocumulonimbus smoke aerosols, *Geophys. Res. Lett.*, 46, 10061–10071, 850 <https://doi.org/10.1029/2019GL082360>, 2019.
- Clark, T., Jenkins, M., Coen, J., and Packham, D.: A coupled atmosphere–fire model: role of the convective Froude number and dynamic fingering at the fireline, *Int. J. Wildland Fire*, 6, 177–190, <https://doi.org/10.1071/WF9960177>, 1996.
- Clements, C. B., et al.: Observing the dynamics of wildland grass fires: FireFlux—A field validation experiment, *Bull. Am. Meteorol. Soc.*, 88, 1369–1382, <https://doi.org/10.1175/BAMS-88-9-1369>, 2007.



855 Cunningham, C. X., Williamson, G. J., and Bowman, D. M.: Increasing frequency and intensity of the most extreme wildfires on Earth, *Nat. Ecol. Evol.*, 8, 1420–1425, 2024.

Cruz, M. G., Alexander, M. E., Sullivan, A. L., Gould, J. S., and Kilinc, M.: Assessing improvements in models used to operationally predict wildland fire rate of spread, *Environ. Model. Softw.*, 105, 54–63, <https://doi.org/10.1016/j.envsoft.2018.03.027>, 2018.

860 Duff, T. J., Chong, D. M., and Penman, T. D.: Quantifying wildfire growth rates using smoke plume observations derived from weather radar, *Int. J. Wildland Fire*, 27, 514–524, <https://doi.org/10.1071/WF17180>, 2018.

Filippi, J.-B., Bosseur, F., Mari, C., and Lac, C.: Simulation of a large wildfire in a coupled fire–atmosphere model, *Atmosphere*, 9, 218, <https://doi.org/10.3390/atmos9060218>, 2018.

865 Filippi, J.-B., Pialat, X., and Clements, C. B.: Assessment of ForeFire/Meso-NH for wildland fire–atmosphere coupled simulation of the FireFlux experiment, *Proc. Combust. Inst.*, 34, 2633–2640, <https://doi.org/10.1016/j.proci.2012.07.022>, 2013.

Fox-Hughes, P., Bridge, C., Faggian, N., Jolly, C., Matthews, S., Ebert, E., Jacobs, H., Brown, B., and Bally, J.: An evaluation of wildland fire simulators used operationally in Australia, *Int. J. Wildland Fire*, 33, WF23028, 2024.

870 Guirguis, K., Hatchett, B., Clemesha, R., et al.: Compound atmospheric drivers of the catastrophic 2025 Los Angeles urban firestorm, *npj Nat. Hazards*, 2, 103, <https://doi.org/10.1038/s44304-025-00155-7>, 2025.

Guyot, A., Brook, J. P., Protat, A., Turner, K., Soderholm, J., McCarthy, N. F., and McGowan, H.: Segmentation of polarimetric radar imagery using statistical texture, *Atmos. Meas. Tech.*, 16, 4571–4588, <https://doi.org/10.5194/amt-16-4571-2023>, 2023.

Jones, R. F.: Radar echoes from smoke, *Meteorol. Mag.*, 79, 933–937, 1950.

875 Jones, T. A. and Christopher, S. A.: Satellite and radar observations of the 9 April 2009 Texas and Oklahoma grassfires, *Bull. Am. Meteorol. Soc.*, 91, 455–460, <https://doi.org/10.1175/2009BAMS2919.1>, 2010a.

Jones, T. A. and Christopher, S. A.: Satellite and radar remote sensing of Southern Plains grass fires: a case study, *J. Appl. Meteorol. Climatol.*, 49, 2133–2146, <https://doi.org/10.1175/2010JAMC2472.1>, 2010b.

880 Jones, M. W., Kelley, D. I., Burton, C. A., Di Giuseppe, F., Barbosa, M. L. F., Brambleby, E., and Xanthopoulos, G.: State of wildfires 2023–2024, *Earth Syst. Sci. Data*, 16, 3601–3685, 2024.



- Kingsmill, D. E., French, J. R., and Lareau, N. P.: In situ microphysics observations of intense pyroconvection from a large wildfire, *Atmos. Chem. Phys.*, 23, 1–21, <https://doi.org/10.5194/acp-23-1-2023>, 2023.
- Kochanski, A. K., Krueger, S. K., Jenkins, M. A., Mandel, J., and Beezley, J. D.: Coupled atmosphere–fire simulations of FireFlux: impacts of model resolution on model performance, arXiv [preprint], <https://doi.org/10.48550/arXiv.1112.0494>, 885 2011.
- Kochanski, A. K., Jenkins, M. A., Mandel, J., Beezley, J. D., Clements, C. B., and Krueger, S.: Evaluation of WRF-SFIRE performance with field observations from the FireFlux experiment, *Geosci. Model Dev.*, 6, 1109–1126, <https://doi.org/10.5194/gmd-6-1109-2013>, 2013.
- Lareau, N. P. and Clements, C. B.: Environmental controls on pyrocumululus and pyrocumulonimbus initiation and 890 development, *Atmos. Chem. Phys.*, 16, 4005–4022, <https://doi.org/10.5194/acp-16-4005-2016>, 2016.
- Lareau, N. P., Donohoe, A., Roberts, M., and Ebrahimian, H.: Tracking wildfires with weather radars, *J. Geophys. Res. Atmos.*, 127, e2021JD036158, <https://doi.org/10.1029/2021JD036158>, 2022.
- Lareau, N. P., Clements, C. B., Kochanski, A., Aydell, T., Hudak, A. T., McCarley, T. R., and Ottmar, R.: Observations of a rotating pyroconvective plume, *Int. J. Wildland Fire*, 33, 2024.
- 895 Liu, Y., et al.: Smoke plume dynamics, in: *Wildland Fire Smoke in the United States*, edited by: Peterson, D. L., McCaffrey, S. M., and Patel-Weynand, T., Springer, Cham, [https://doi.org/10.1007/978-3-030-87045-4\\_4](https://doi.org/10.1007/978-3-030-87045-4_4), 2022.
- Mankins, J. C.: *Technology readiness levels*, 1995.
- May, P. T., Guyot, A., Protat, A., and Curtis, M.: Accuracy of polarimetric radar ZDR estimates: implications for the quantitative observation of meteorological and nonmeteorological echoes, *J. Atmos. Oceanic Technol.*, 41, 621–628, 900 <https://doi.org/10.1175/JTECH-D-23-0122.1>, 2024.
- Mass, C. F. and Ovens, D.: The meteorology of the August 2023 Maui wildfire, *Weather Forecast.*, 39, 1097–1115, <https://doi.org/10.1175/WAF-D-23-0210.1>, 2024.
- McCarthy, N., McGowan, H., Guyot, A., and Dowdy, A.: Mobile X-Pol radar: a new tool for investigating pyroconvection and associated wildfire meteorology, *Bull. Am. Meteorol. Soc.*, 99, <https://doi.org/10.1175/BAMS-D-16-0118.1>, 2018.
- 905 McCarthy, N., Guyot, A., Dowdy, A., and McGowan, H.: Wildfire and weather radar: a review, *J. Geophys. Res. Atmos.*, 124, 266–286, <https://doi.org/10.1029/2018JD029285>, 2018.



- McCarthy, N. F., Guyot, A., Protat, A., Dowdy, A. J., and McGowan, H.: Tracking pyrometeors with meteorological radar using unsupervised machine learning, *Geophys. Res. Lett.*, 47, <https://doi.org/10.1029/2019GL084305>, 2020.
- McCarthy, N. F., McGowan, H., Guyot, A., Dowdy, A., Sturgess, A., and Twomey, B.: Crown fire initiation of a  
910 thunderstorm, *Int. J. Wildland Fire*, 32, 545–560, <https://doi.org/10.1071/WF21146>, 2023.
- McGowan, H., Guyot, A., Seifried, V., and Soderholm, J.: Observations of a frontal–trough merger over a wildfire, Queensland, Australia, *Q. J. R. Meteorol. Soc.*, 151, e5012, <https://doi.org/10.1002/qj.5012>, 2025.
- McGowan, H., Guyot, A., Sturman, A., Seifried, V., and Dale, T.: Observations of wildfire–atmosphere interactions over mountainous terrain, southeast Queensland, Australia, *J. Appl. Meteorol. Climatol.*, in press, [https://doi.org/10.1175/JAMC-  
D-25-0119.1](https://doi.org/10.1175/JAMC-<br/>915 D-25-0119.1), 2026.
- Protat, A., Louf, V., and Brook, J. P.: SWIRL: the first Australian operational radar-based 3D wind analysis system, *J. Atmos. Oceanic Technol.*, 41, 725–746, <https://doi.org/10.1175/JTECH-D-23-0155.1>, 2024.
- McRae, R. H., Sharples, J. J., and Fromm, M.: Linking local wildfire dynamics to pyroCb development, *Nat. Hazards Earth Syst. Sci.*, 15, 417–428, 2015.
- 920 Melnikov, V. M., Zrnica, D. S., and Rabin, R. M.: Polarimetric radar properties of smoke plumes: a model, *J. Geophys. Res.*, 114, D21204, <https://doi.org/10.1029/2009JD012647>, 2009.
- Melnikov, V. M., Zrnica, D. S., Rabin, R. M., and Zhang, P.: Radar polarimetric signatures of fire plumes in Oklahoma, *Geophys. Res. Lett.*, 35, L14815, <https://doi.org/10.1029/2008GL034311>, 2008.
- Mirkovic, D., Stepanian, P. M., Wainwright, C. E., Reynolds, D. R., and Menz, M. H.: Characterizing animal anatomy and  
925 internal composition for electromagnetic modelling in radar entomology, *Remote Sens. Ecol. Conserv.*, 5, 169–179, 2019.
- Mirkovic, D., Zrnica, D. S., Melnikov, V., and Zhang, P.: Effects of rough hail scattering on polarimetric variables, *IEEE Trans. Geosci. Remote Sens.*, 60, 1–14, 2021.
- Palumbo, R. A., Al-Ashwal, W. A., Ferguson, B., McCarroll, C., and McLaughlin, D. J.: Weather and bushfire observation using low-cost X-band phased array radars, in: *Proc. Int. Radar Conf.*, 2013.
- 930 Palumbo, R. A.: Applications in low-power phased array weather radars, 2016.



- Peace, M., Mattner, T., Mills, G., Kepert, J., and McCaw, L.: Coupled fire–atmosphere simulations of the Rocky River fire using WRF-SFIRE, *J. Appl. Meteorol. Climatol.*, 55, 1151–1168, <https://doi.org/10.1175/JAMC-D-15-0157.1>, 2016.
- Peace, M., McCaw, L., Santos, B., Kepert, J. D., Burrows, N., and Fawcett, R. J. B.: Meteorological drivers of extreme fire behaviour during the Waroona bushfire, Western Australia, *J. South. Hemisph. Earth Syst. Sci.*, 67, 79–106, 935 <https://doi.org/10.22499/3.6702.002>, 2018.
- Peace, M., Ye, H., Greenslade, J., and Kepert, J. D.: The destructive Sir Ivan fire in New South Wales, Australia: simulations using a coupled fire–atmosphere model, *Fire*, 6, 438, 2023.
- Peterson, D. A., Campbell, J. R., Hyer, E. J., et al.: Wildfire-driven thunderstorms cause a volcano-like stratospheric injection of smoke, *npj Clim. Atmos. Sci.*, 1, 30, <https://doi.org/10.1038/s41612-018-0039-3>, 2018.
- 940 Potter, B. E.: Atmospheric interactions with wildland fire behaviour – I. Basic surface interactions, vertical profiles and synoptic structures, *Int. J. Wildland Fire*, 21, 779–801, 2012.
- Potter, B. E.: Atmospheric interactions with wildland fire behaviour – II. Plume and vortex dynamics, *Int. J. Wildland Fire*, 21, 802–817, 2012.
- Price, O. F., Purdam, P. J., Williamson, G. J., and Bowman, D. M. J. S.: Comparing the height and area of wild and 945 prescribed fire particle plumes in south-east Australia using weather radar, *Int. J. Wildland Fire*, 27, 525–537, <https://doi.org/10.1071/WF17166>, 2018.
- Rogers, R. R. and Brown, W. O. J.: Radar observations of a major industrial fire, *Bull. Am. Meteorol. Soc.*, 78, 803–814, [https://doi.org/10.1175/1520-0477\(1997\)078<0803:ROOAMI>2.0.CO;2](https://doi.org/10.1175/1520-0477(1997)078<0803:ROOAMI>2.0.CO;2), 1997.
- Skamarock, W. C.: Positive-definite and monotonic limiters for unrestricted-time-step transport schemes, *Mon. Weather 950 Rev.*, 134, 2241–2250, <https://doi.org/10.1175/MWR3170.1>, 2006.
- Soderholm, J., McGowan, H., Richter, H., Walsh, K., Weckwerth, T., and Coleman, M.: The Coastal Convective Interactions Experiment (CCIE): understanding the role of sea breezes for hailstorm hotspots in eastern Australia, *Bull. Am. Meteorol. Soc.*, 97, 1687–1698, 2016.
- Sun, J., Speer, K., Quaife, B., Cai, M., and Schwartzman, D.: The ceiling height of wildland fire plumes in sheared boundary 955 layer flow, *arXiv [preprint]*, <https://arxiv.org/pdf/2501.08343>, 2025.

<https://doi.org/10.5194/egusphere-2026-2256>

Preprint. Discussion started: 13 May 2026

© Author(s) 2026. CC BY 4.0 License.



Terrasson, A., McCarthy, N., Dowdy, A., Richter, H., McGowan, H., and Guyot, A.: Weather radar insights into the turbulent dynamics of a wildfire-triggered supercell thunderstorm, *J. Geophys. Res. Atmos.*, 124, 8645–8658, <https://doi.org/10.1029/2018JD029986>, 2019.

960 Wurman, J. and Weygandt, S.: Mobile radar observations of the Big Elk (2002) and Roberts (2003) fires, in: 5th Symp. Fire For. Meteorol., 2003.